ELSEVIER

Marine and Petroleum Geology 23 (2006) 145–164

Marine and Petroleum Geology

www.elsevier.com/locate/marpetgeo

Characterisation and correlation of active hydrocarbon seepage using geophysical data sets: An example from the tropical, carbonate Yampi Shelf, Northwest Australia

N. Rollet *, G.A. Logan, J.M. Kennard, P.E. O'Brien, A.T. Jones, M. Sexton

Geoscience Australia, GPO Box 378, Canberra ACT 2601, Australia

Received 25 April 2005; received in revised form 22 September 2005; accepted 1 October 2005

Abstract

For the first time in Australia, active present-day hydrocarbon seepage has been imaged—on the tropical carbonate Yampi Shelf, in 50 and 90 m water depth. Seepage is evidenced by gas plumes in the water column that are associated with seabed features, such as clusters of reflective blocks, hard-grounds, pockmark fields, and mounds. Seepage activity and intensity seems to vary with changes in pressure related to macro-tidal cycles. The seabed features coincide with sub-surface features such as areas of seismic signal attenuation under high amplitude reflectors, seismic discontinuities and bright spots. Hydrocarbon migration-seepage pathways appear to be controlled by the reactivation of pre-existing fractures and dykes within the basement. The types of seabed features and their preservation on a tropical carbonate shelf are strongly influenced by the coarse bioclastic nature of sediments and the high energy of macro-tidal currents and storm reworking.

Keywords: Seep detection; Hydrocarbon leakage; Pockmarks; Carbonate mounds

1. Introduction

1.1. Active seeps detection—a tool for hydrocarbon exploration

The presence of hydrocarbon seeps in either near-surface sediments, on the seabed, or within the water column, may provide strong evidence of an active petroleum system. Indeed, the detection of seepage has been used in offshore oil and gas exploration since the 1930s (Abrams and Segall, 2001). However, the complexity of hydrocarbon leakage and seepage in a particular marine setting requires understanding substrate features and geochemical processes (Abrams and Segall, 2001). During the past decade, a renewed interest has developed in geochemical seepage exploration assisted by the development of new analytical and interpretative methods (Schumacher, 2000; Abrams and Segall, 2001).

The North West Shelf (NWS) of Australia (Fig. 1) is a world class gas province with significant oil sweet spots (Longley et al., 2002). In the northern part of the NWS, on the Yampi Shelf and Timor Sea region (Fig. 1), extensive palaeo-hydrocarbon leakage and present-day hydrocarbon seepage have been inferred from seismic attribute analysis, remote sensing data sets (Synthetic Aperture Radar—SAR, Airborne Laser Fluoro-sensor—ALF), and water column geochemical sniffer (Jones et al., 2005a; O'Brien and Woods, 1995; O'Brien et al., 2000, 2001, 2002a,b, 2003a).

This study investigated the nature of the inferred seepage on the Yampi Shelf (Fig. 1) during Geoscience Australia marine survey S267 (Logan, 2004; Jones et al., 2005a). The survey was undertaken to test a combination of tools and techniques in an area of inferred seepage prior to the deployment of tools for seepage detection in more poorly understood areas and frontier basins.

1.2. Hydrocarbon seepage in shallow marine environments

Fluid seepage from the seafloor has been reported in many locations around the world in different water depths, from 10 to 3000 m. In shallow and moderate water depths, between 10 and 500 m, the fluids involved in seepage can be of various origins (groundwater, biogenic or thermogenic), with different intensity (macro- vs micro-seepage), and

* Corresponding author. Tel.: +61 2 6249 9165; fax: +61 2 6249 9915.
E-mail address: nadege.rollet@ga.gov.au (N. Rollet).

0264-8172/$ - see front matter © 2005 Published by Elsevier Ltd.
doi:10.1016/j.marpetgeo.2005.10.002

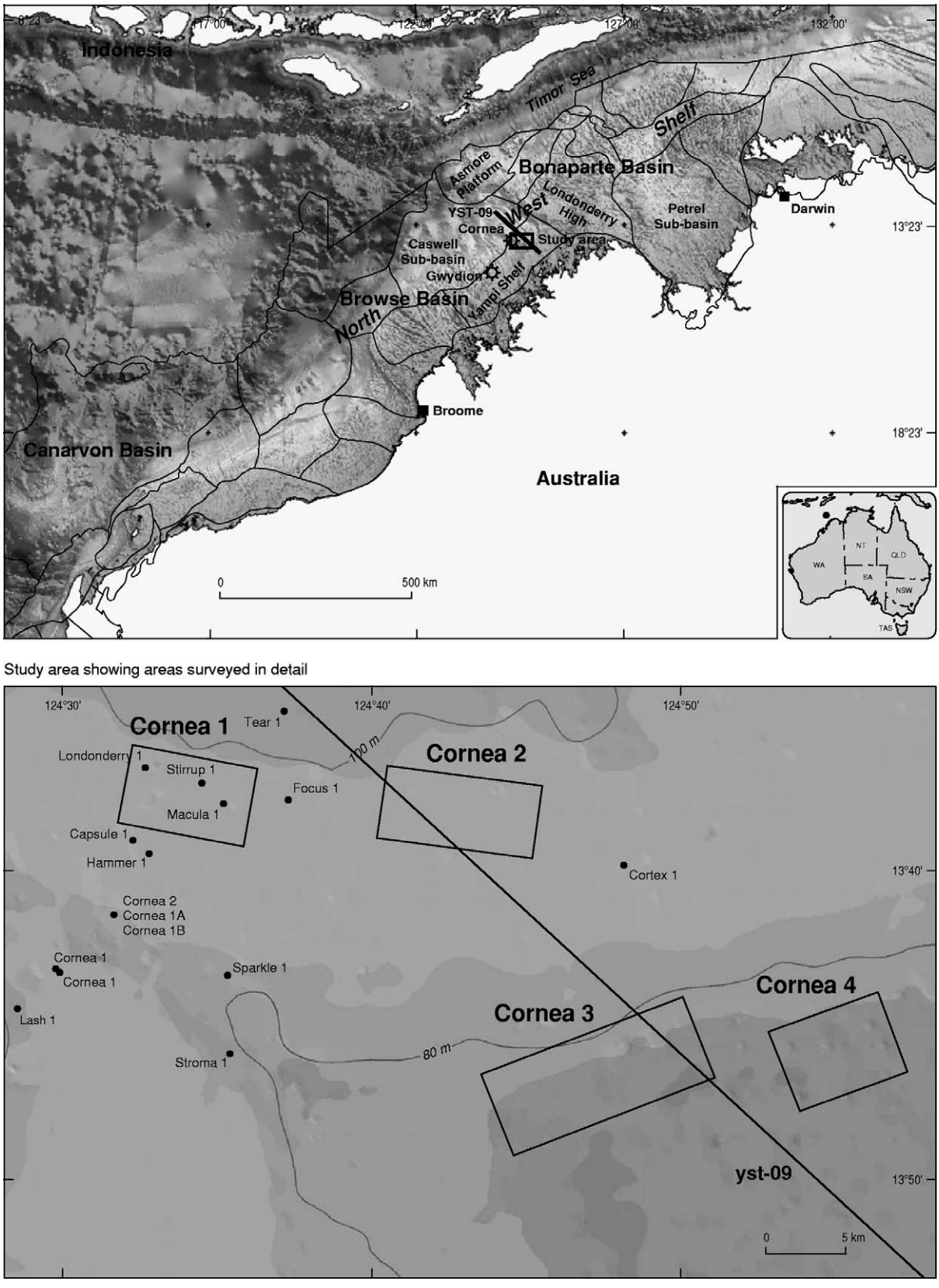

Fig. 1. Regional setting of the study area on the Yampi Shelf. White lines indicate geological province boundaries; background 1 km bathymetry map is derived from swath, predicted satellite, levelled survey track data and hydrographic charts. Wells drilled in the study areas are indicated. The seismic line YST-165-09 is located north of the Cornea oil and gas field and is shown in Fig. 2.

Table 1
Location, depth, environment and tectonic setting of key features related to seepage in shallow-moderate water depths around the world

Location	Water depth	Environment and tectonic setting	Features related to seepage	References
Eastern Mediterranean	20–80 m	Siliciclastic (silt, sandy-silt), sub-tropical, compressive system	Gas bubbles, pockmarks and acoustic anomalies	Hasiotis et al. (1996); Christodoulou et al. (2003); Garcia-Garcia et al. (2004)
Western Indian margin	20–260 m	Siliciclastic (silt, clay, sand), tropical, passive margin	Gas plumes, pockmarks and acoustic masking	Karisiddaiah and Veerayya (2002)
Timor Sea Region, Northwest Australia	40–500 m	Carbonate, tropical, passive margin–early collisional margin	Remote sensing (SAR and ALF) and 2D/3D seismic anomalies combined with high-resolution bathymetry features	Bishop and O'Brien (1998) and O'Brien et al. (2002a,b, 2003a)
Yellow Sea, East China	80–100 m	Siliciclastic (palimpsest sand), sub-tropical, inverted extensional basin	Gas plumes, craters with rare pockmarks and diapirs associated with seismic wipeout	Jeong et al. (2004)
North Sea, UK sector	<100–250 m	Siliciclastic (silty marine clays, glaciomarine silts), temperate, Sag margin with inversion and salt movement	Gas plumes and/or sediment clouds suspended in the water column, pockmarks, authigenic carbonates and bacterial mats	Hovland and Judd (1988); Judd (2001); Judd et al. (2002); Loseth et al. (2003)
East China Sea	<100–1000 m	Siliciclastic (mud), sub-tropical, back-arc basin	Mud volcanoes, large pockmarks, bright spots, phase inversion and other seismic anomalies	Yin et al. (2003)
Lake Baikal	<100–1500 m	Siliciclastic (coarse sandy turbidites), desertic, rift system.	Methane seeps, mud cones, low relief craters and gas hydrates	Van Rensbergen et al. (2003)
Black Sea	<100–2000 m	Siliciclastic, sub-tropical, compressional setting	Gas plumes, gas-saturated-sediments, gas hydrates, mud volcanoes and pockmarks	Ergün et al. (2002); Kruglyakova et al. (2004)
Offshore Canning Basin, Northwest Australia	<100–3000 m	Carbonate, tropical, passive margin	Remote sensing (SAR and ALF) and 2D seismic anomalies	O'Brien et al. (2003b)
Bering Sea	<200 m	Siliciclastic, polar, convergent margin	Gas bubbles in the water column, pockmarks, and seismic wipeout zone related to gas	Abrams (1992)
East Atlantic (Gulf of Cadiz)	300–400 m	Siliciclastic (mud), sub-tropical, compressional system	Gas plumes, ancient and modern pockmarks, acoustic turbidity and blanking, bright spots and bottom simulating reflector	Casas et al. (2003)
Caspian Sea	<400–1000 m	Siliciclastic (mud), sub-tropical, compressional system	Mud volcanoes	Yusifov and Rabinowitz (2004)
West African margin	<400–3000 m	Siliciclastic (sand/silt), tropical, passive margin	Pockmarks	Hovland et al. (1997); Gay et al. (2003)

observed in a variety of sedimentary, climatic and tectonic settings (Table 1).

Most published studies of seepage are in siliciclastic-dominated environments and evidence of hydrocarbon seeps is often associated with mud volcanoes or mud domes (e.g. several tens of meters high to more than 200 m high in the Caspian Sea, Yusifov and Rabinowitz, 2004) or pockmarks (circular or elliptical depressions <0.5–20 m deep and from 1 to 1000 m long in the North Sea, Hovland and Judd, 1988; and up to 58 m deep in the Gulf of Mexico, Prior et al., 1989). Mud volcanoes are more common within active accretionary prisms or other compressional settings where active fluid dynamics, including de-watering, are important. In contrast, pockmarks have been widely reported in various tectono-stratigraphic settings often associated with structural or stratigraphic discontinuities (unconformities along bedrock, Shaw et al., 1997; faults and folded anticlines, Eichhubl et al., 2000; salt diapirs, Taylor et al., 2000; shallow buried channels, Gay et al., 2003), but are mainly found in unconsolidated fine-grained siliciclastic sediments (Hovland and Judd, 1988; Judd, 2001).

Methane-derived authigenic carbonates (MDACs) or hydrocarbon-related diagenetic zones (HRDZs) have been associated with palaeo- and/or present-day seepage either on the seabed or within the underlying stratigraphic section (Hovland and Judd, 1988; O'Brien and Woods, 1995). MDACs and HRDZs are the result of hydrocarbon leakage and biogeochemical (microbial) processes in overlying shallow aquifers (Cowley and O'Brien, 2000) or on the seabed. The coupling of sulphate reduction with methane oxidation can produce intense carbonate cementation (Boetius et al., 2000). The high acoustic impedance produced by this cementation provides a strong seismic response (Cowley and O'Brien, 2000). Such carbonate-cemented sediments have also been found inside large pockmarks in the North Sea (Hovland et al., 1985; Dando et al., 1991). Generally, seabed authigenic carbonates are rapidly colonised by bacterial mats and chemosynthetic fauna (Hovland, 1990; Stakes et al., 1999). These methane-derived carbonates, generally classified as hard-grounds, form durable substrates. They could represent the initial phase of bioherm and carbonate reef formation in

warmer waters, and following burial may also form reservoirs (Hovland, 1990).

1.3. Inferred hydrocarbon seepage on the tropical carbonate Yampi Shelf

On the tropical carbonate Yampi Shelf, sea-level change and reef development in conjunction with powerful hydraulic forces (storms and swells, tropical cyclones, major ocean currents and tides) have controlled the modern bathymetry and sedimentology (O'Brien and Glenn, 2005). In addition, seaward-flowing saline bottom waters, generated by seasonal evaporation on the upper shelf, significantly limit modern benthic carbonate production on most of the middle shelf (James et al., 2004). Therefore, bioclastic carbonate sediments on the shelf are deposited with a low or starved sedimentation rate (Van Andel and Veevers, 1967; Marshall et al., 1994), which is not favourable for the formation of the large-scale seepage features (mud volcanoes and mature pockmarks) observed in fine-grained siliciclastic environments around the world (Table 1). Instead, possible seepage-related features observed in the Timor Sea are occasional small pockmarks (2–5 m in diameter), seabed mounds, carbonate banks, reefs or shoals (Heyward et al., 1997; Hovland et al., 1994; Lavering and Jones, 2001; O'Brien and Glenn, 2005).

Late Tertiary collision of the Australian and Eurasian plates has generated a compressional regime on the NWS and culminated in a major phase of Late Miocene–Recent foreland subsidence and widespread extensional reactivation of existing faults in the Timor Sea area (Etheridge et al., 1991; O'Brien et al., 1999b; Keep et al., 2002). This recent faulting is considered the major cause for numerous breached hydrocarbon traps in the region (O'Brien et al., 1996,1999a,b). It has also been proposed that many of the carbonate bank systems within the Timor Sea have developed over active hydrocarbon seeps (Hovland et al., 1994; Heyward et al., 1997; Lavering and Jones, 2001; Glenn and O'Brien, 2002; Longley et al., 2002; O'Brien and Glenn, 2005). In this high-energy tropical carbonate environment, reefs could rapidly develop on any topographic highs formed by seepage-related features where authigenic carbonate cementation is pronounced and where the terrain is swept by strong currents that supply nutrients and oxygen (Hovland, 1990).

Prolific present-day seepage has been inferred in the Timor Sea region on the NWS based on synthetic aperture radar (SAR), airborne laser fluorescence (ALF), geochemical water column sniffer studies and 2D seismic data (O'Brien and Woods, 1995; O'Brien et al., 1996, 1999b, 2001, 2002a,b, 2003a; Bishop and O'Brien, 1998) and 3D seismic studies (Shell Development (Australia) Pty. Ltd., 2000). However, recent reassessment of the potential origin of SAR slicks in the area has downgraded the abundance and distribution of present-day hydrocarbon seepage in favour of alternative slick origins, such as bathymetrically controlled current flow and coral spawning (Jones et al., 2005a). Also, palaeo- and present-day hydrocarbon migration and seepage cannot always be distinguished on seismic data alone. 3D seismic data indicate that the onset of reef growth in the Timor Sea coincides with the timing of both Pliocene subsidence and trap breach (O'Brien and Glenn, 2005). However, present-day seepage has not been confirmed, apart from a few isolated areas with elevated methane and ethane concentrations and 'fluorescence' in the water column (Edwards and Crawford, 1999; O'Brien et al., 2000). Therefore, seabed imaging and further field studies are necessary to demonstrate any unequivocal relationships between seabed features and present-day active hydrocarbon seepage on the NWS.

The objectives of this paper are: (1) to describe, characterise and discuss the relevance of using an integrated approach for the detection of active seepage, (2) to correlate relevant data to explain seepage and (3) to compare the range of seepage features on a shallow carbonate shelf with those observed in siliciclastic environments.

2. Database and methods

2.1. Previously existing data

Four areas on the Yampi Shelf were selected for surveying in the vicinity of the Cornea oil and gas field (Fig. 1). A range of previously existing data sets were used to identify areas of likely active seepage. These included SAR, Landsat and sniffer surveys together with broad bathymetry, 2D and 3D seismic surveys and 3.5 kHz sub-bottom profiles. Such data were assessed for evidence of surface slicks, water column and sub-surface sediment gas, seafloor pockmarks and mounds, and seismic expression of hydrocarbon migration, accumulation and leakage. All data sets were integrated within a geographic information system (GIS) and four areas of interest were high-graded for survey and sample collection during GA Survey 267 (Jones et al., 2005b). Each survey area contains multiple lines of evidence for seepage including:

- Interpreted hydrocarbon-related diagenetic zones (HRDZs) mapped in the Cornea 3D seismic grid (Shell Development (Australia) Pty. Ltd., 2000);
- High amplitude of the seafloor reflector extracted from 2D (Cowley and O'Brien, 2000) and 3D seismic data;
- High concentrations of methane (300 ppm, 75–100 times background values) and ethane (>2 ppm) in the water column (O'Brien et al., 2000, 2001);
- ALF anomalies (Cowley and O'Brien, 2000);
- SAR slicks (O'Brien et al., 2003a; Jones et al., 2005a);
- Landsat slicks (Cook, 2000);
- ARGUS hyperspectral slicks (Fugro Airborne Surveys Pty Ltd., 2001);

2.2. New data on the Yampi Shelf

Geoscience Australia marine survey S267 was carried out over the Yampi Shelf to test and validate a range of techniques for seep detection in March 2004 (Fig. 1). It used a combination of tools including side-scan sonar (Klein 540 dual frequency with 100 and 500 kHz transducers recorded digitally), echo-sounders (screen

images of two 200 kHz units located near the bow and stern, approximately 10 m apart, were captured with a digital camera), multi-beam bathymetric mapping (two LSE-296 transducer arrays connected to a SEE-30 Transmit/Receive Unit operating at 180 kHz) and a sea-surface fluorescence device. A sampling program was then carried out over areas of interest to collect sediment and water samples for sedimentological, geochemical and biological analysis. The survey was undertaken on the vessel *Parmelia K*, a pearling boat that forms part of the Broome Pearls fleet. This vessel was positioned using standard GPS satellite navigation. The average survey speed was 5–6 knots with the sonar towfish situated between 130 and 240 m behind the ship, approximately 40 m above the seabed. Side-scan sonar mosaics were generated over the areas incorporating layback correction giving an accuracy of several meters for the location of the sonar towfish. Full details of the survey are presented in the post cruise report (Jones et al., 2005b).

During Survey 267, approximately 158 km^2 of multi-beam swath bathymetry data, 770 km of side-scan sonar data, 16 grab samples, 12 dredge samples and 3 gravity cores were collected. Echo-sounder data were also examined throughout the survey. Existing 2D and 3D seismic data were examined before the survey and were subsequently correlated with the newly acquired data.

Core material was difficult to obtain in the sandy and locally cemented sediments using 2 and 4 m gravity cores. Sampling using a Smith–MacIntyre grab and dredges was highly successful, with samples taken within the immediate vicinity of active seeps. Detailed analysis of sediment samples collected during the survey is beyond the scope of this paper. The sampling revealed that grabs generally returned light olive-grey, bioclastic carbonate muddy sand, while dredges retrieved coarser sediment and hard-ground fragments (with fines winnowed in the water column during sample retrieval).

A selection of light and dark coloured carbonate samples (shells, worm tubes, crusts and pebble-sized aggregates) were analysed for their mineralogy (by Laser Raman microprobe) and for carbonate isotopes. Stable isotope ratios were measured at Monash University using a Finnigan MAT 252 mass spectrometer (I. Cartwright, pers. comm., 2005).

3. Regional geology

The NWS is a proven hydrocarbon province but no production has yet been undertaken on the Yampi Shelf despite the discoveries of hydrocarbons. The Yampi Shelf forms the eastern flank of the northern Browse Basin and adjoins the Caswell Sub-basin depocentre to the west (Fig. 1). The basinward limit of the shelf is characterised by normal faulting. The shelf is an area of shallow, gently basinward dipping Proterozoic basement (Fig. 2). This basement is mainly igneous (rhyolite, rhyodacite, gabbro, granite) with local

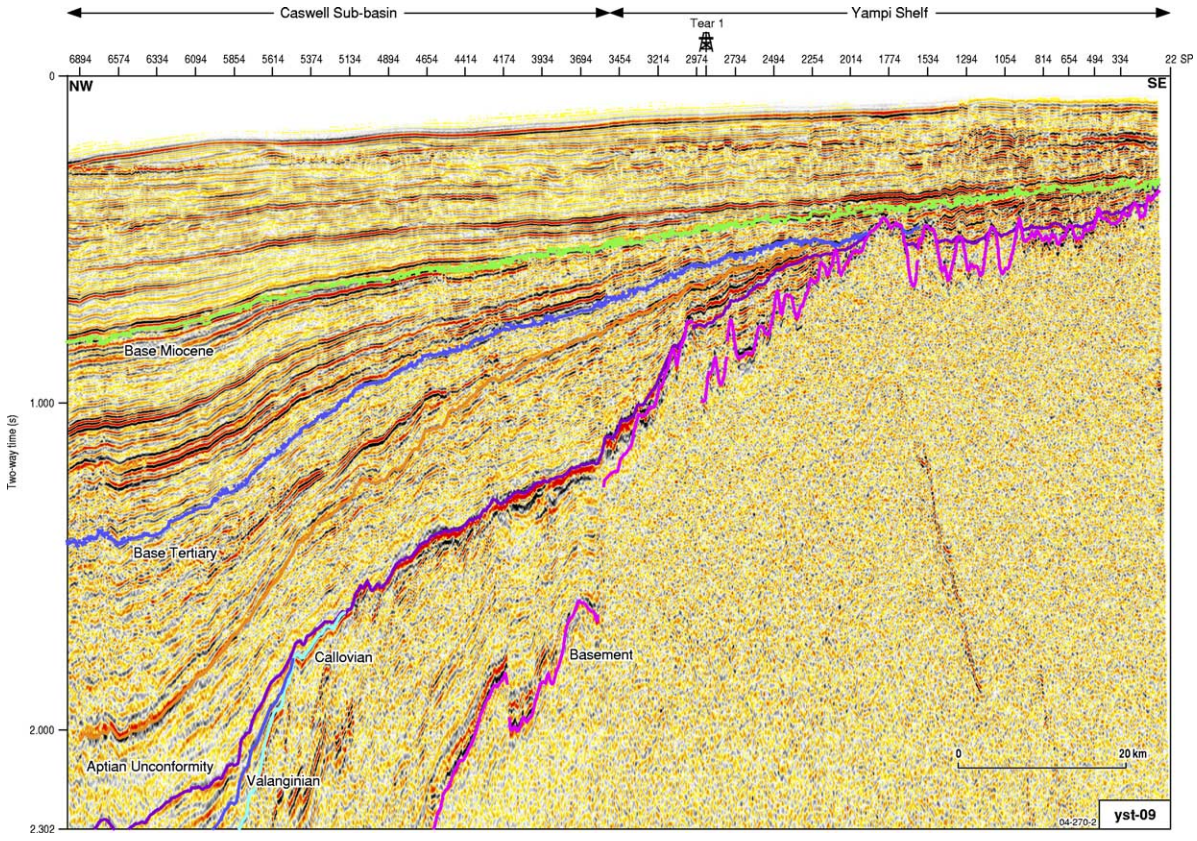

Fig. 2. 2D seismic GA line YST-165-09 showing interpreted stratigraphy from the Caswell Sub-basin to the Yampi Shelf (location in Fig. 1). The location of Tear-1 well is indicated here and in Fig. 1.

quartzite and is highly eroded with rugose palaeo-topographic relief. It is overlain by a 40 m thick basal conglomerate which consists of igneous pebbles in a very fine pyritic groundmass and is interbedded with arkosic sandstones. Proterozoic basement is onlapped by Permian to Mesozoic sediments. The Palaeozoic sediments have been uplifted, progressively eroded and overlain by an easterly onlapping and thinning wedge of Late Jurassic, Cretaceous and Tertiary sediments (Struckmeyer et al., 1998). Total sediment thickness on the shelf is less than 1000 m.

The Late Cretaceous–Cainozoic section records a major progradational (regressive) cycle in which the shelf edge migrated northwestwards from the Yampi Shelf to the outer limits of the Caswell Sub-basin. In the Oligocene, mild uplift and erosion occurred over much of the shelf, and accelerated subsidence of the outer shelf led to the deposition of a thick prograding carbonate wedge and establishment of the present morphology of the shelf and slope (Willis, 1988). Inversion of some Palaeozoic–Jurassic faults commenced in the Middle to Late Miocene as a result of convergence and collision of the Australian and Eurasian plates (Struckmeyer et al., 1998).

Biodegraded oil and gas discoveries at Gwydion (Spry and Ward, 1997) and Cornea (Ingram et al., 2000), currently considered uneconomic, have validated the existence of a petroleum system sourced in the Early Cretaceous, and indicate that the Yampi Shelf is favourably situated to receive charge from the mature source rocks within the adjacent Caswell Sub-basin (Blevin et al., 1998). This depocentre contains in excess of 15 km of Late Palaeozoic–Mesozoic strata, but the regional northwesterly dip on the Yampi Shelf limits the potential for structural hydrocarbon traps (Spry and Ward, 1997).

The Yampi Shelf lies at water depths of 40 to 100 m and was exposed at the Last Glacial Maximum [Pleistocene, approximately 19,000 (calendar) yrs BP; Yokoyama et al., 2000].

4. Evidence for seepage

4.1. Plumes in the water column

The echo-sounder and side-scan sonar datasets are very significant as they represent the first direct imaging of seepage in the region, which has previously only been interpreted indirectly. A subsequent survey (SS06/05) on MRV Southern Surveyor during June 2005 directly sampled the plumes within the survey area discussed in this manuscript (Brunskill, 2005, http://www.marine.csiro.au/nationalfacility/voyagedocs/index.htm). The plumes have been shown to be mostly composed of methane with minor amounts of ethane (K. Burns, Australian Institute of Marine Science, pers. comm. 2005).

4.1.1. Echo-sounder

Active seepage over Cornea areas 1 and 2 was initially imaged using echo-sounders. Echo-sounder images of seepage varied considerably—from vertical to inclined plumes aligned with tidal currents (Fig. 3). The active plumes rise to 30–50 m above the sea floor and appear to 'plateau-out' along a sub-horizontal layer, in 40–60 m water depth (Fig. 3), possibly

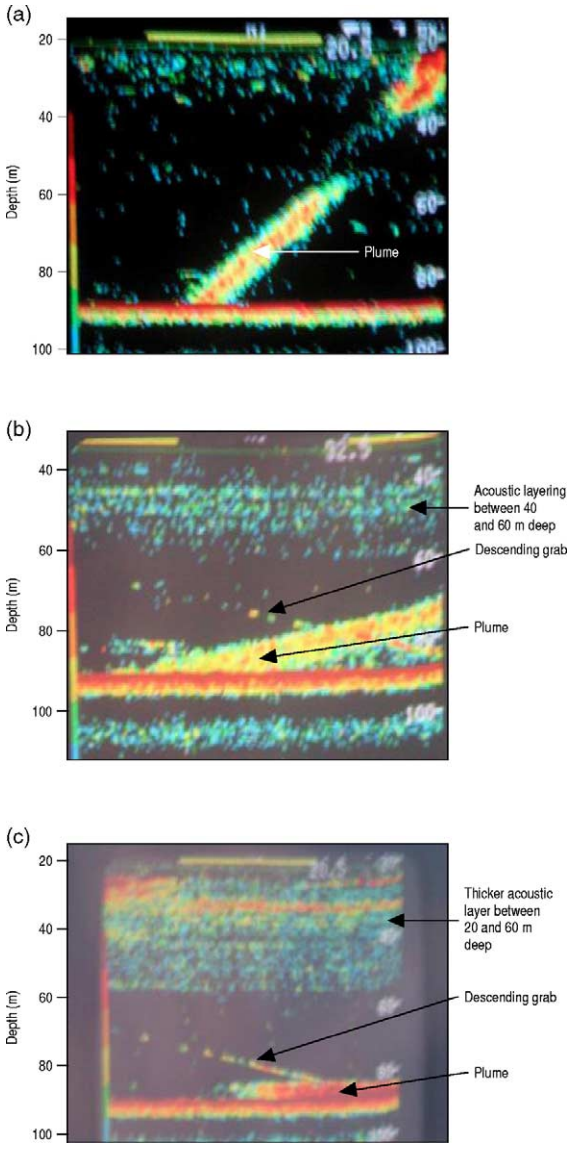

Fig. 3. Echo-sounder screen photos imaging gas plumes in the water column. (a) Shows a discontinuous plume, (b) illustrates several plumes and acoustic layering between 60 and 40 m depth, (c) images a direct grab sampling of a seep.

following an iso-density surface in the water column (most likely a stable thermocline) or an oceanic methane layer formed when particles lifted by bubbles are abandoned when the bubbles dissolve, which often happens at the thermocline (Leifer and Judd, 2002). Because temperature and salinity data, at and beneath this layer, were not obtained during the survey, the nature of the layer (thermocline and/or halocline) could not be defined during the survey. However, a recent study undertaken on the NWS (James et al., 2004) shows that during summer (close to the time at which the data were acquired) the waters in the region are well stratified, with a shelf thermocline between 30 and 60 m water depth, which is consistent with the observations made during the survey. This layering in the water column was not visible over all the survey area and may have been accentuated on the echo-sounder where gas bubbles were trapped along the thermocline.

The echo-sounder was also used extensively to position the survey vessel for accurate sampling of seepage areas, since it was possible to simultaneously observe the plumes rising from the sea-floor and the sample tools as they were lowered to the seabed (Fig. 3).

4.1.2. Side-scan sonar

Side-scan sonar data were also critical for the detection of hydrocarbon seeps on the Yampi Shelf. The side-scan sonar was able to image plumes of high back-scatter material streaming from active seeps in Cornea areas 1 and 2 (Fig. 4). The side-scan data were presented and stored as 'normal' side-scan images, that is, high backscatter appears as dark on the record. Active seeps were particularly well imaged by the 100 kHz transducer on the starboard side; the port transducer data were of poorer quality. These plumes show a high backscatter which could be interpreted as mainly gas (De Beukelaer et al., 2003). During our survey, gas bubbles reached the sea surface at one location, where they had an estimated 1 cm diameter and burst with a very thin oily film.

In the side-scan sonar data, bubble plumes appear as multiple streams of bubbles sloping upward in the direction of the tidal current or as overlapping hyperbolic streams (Fig. 4), which appear to arch up through the water column and then dip downwards. Similar hyperbolic responses have been recognised in sonar records of seepage plumes in the Gulf of California (Merewether et al., 1985). These arched anomalies may result from a combination of: (1) bubble plumes streaming away from the vertical plane traced by the side-scan fish; (2) plumes streaming through the horizontal plane traced by the fish; (3) a curved plume that streams vertically from the seabed and then horizontally along an iso-density surface, as observed in the echo-sounder data. The relatively straight responses are the result of plumes streaming perpendicular to, parallel to, or towards the vertical plane traced by the side-scan fish, but which do not rise above the depth of the fish's horizontal track.

4.2. Seabed features related to active seepage

Side-scan data also provided information on the seabed expression of these seeps, which was often highly variable (Figs. 4 and 5). The side-scan data, as well as the multi-beam bathymetry, were collected along parallel lines about 300 m apart. The line spacing allowed an overlap of swaths for the multi-beam bathymetry. The side-scan sonar swath width is generally half that of the multi-beam bathymetry, so side-scan sonar mosaics do not show a full coverage of the surveyed areas. Nevertheless, geo-referenced side-scan sonar mosaics allow direct correlation among the different sets of data in the surveyed areas.

4.2.1. Side-scan sonar seabed features

Various seabed features are associated with gas seeps in Cornea areas 1 and 2 (Fig. 5). The most common features are clusters of hard, reflective blocks (each block is roughly 1-m in diameter) which are often arranged in a circular ring, possibly around the vent (Fig. 5a–c). They are associated with observed

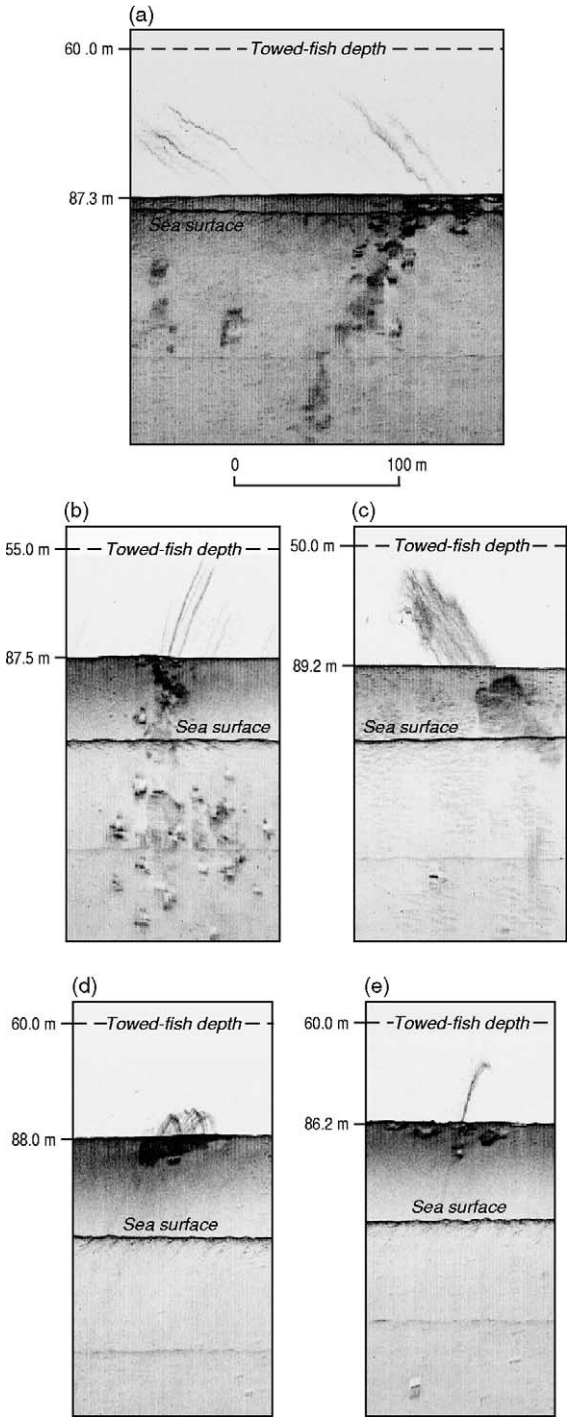

Fig. 4. Side-scan sonar data illustrating gas plumes into the water column. (a–c) Linear plumes are sloping upward in the direction of the tidal current, up to a layer between 60 and 40 m depth, which was observed on the ships' echo-sounder (d,e) hyperbolic-shaped plumes are reaching up to 20 m above the seafloor.

plumes of material in the water column (Fig. 4). The nature of these strong reflective blocks is not proven although dredges taken over seepage areas often retrieved fragments of crusts of cemented bioclastic material. Other common features are larger, hard, reflective hard-grounds and mounds of varying size and shape that appear as bright irregular patches on

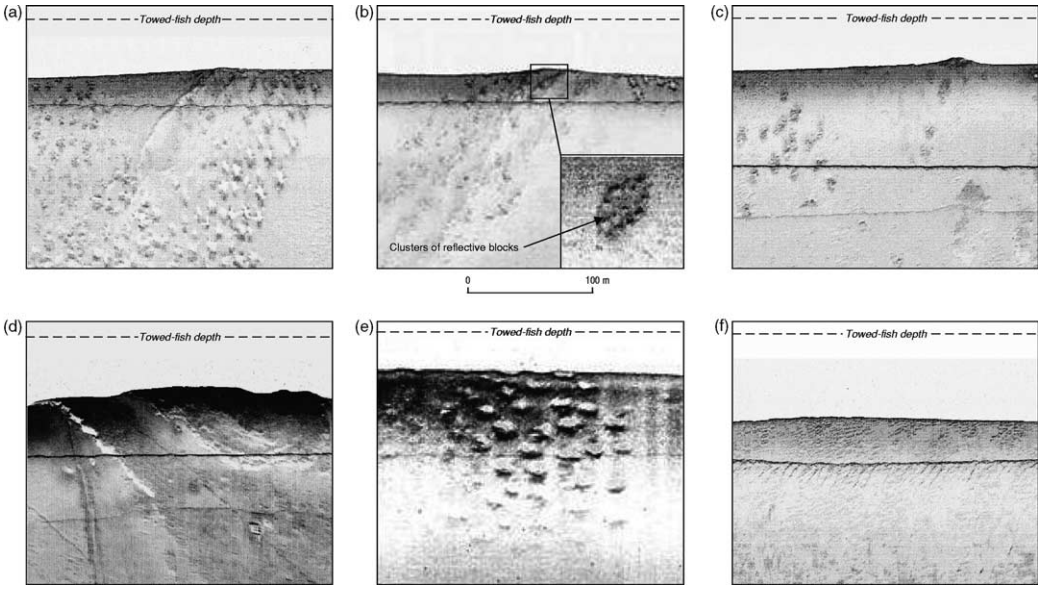

Fig. 5. Side-scan sonar images (starboard only) of seabed features related to seepage in Cornea areas 1, 2 and 4. (a,b) Clusters of strong reflective blocks aligned on a linear trend, (c) clusters of strong reflective blocks and a cemented mound, (d) a reflective hardground, (e) a pockmark field, (f) ripples on the seabed suggesting recent seabed current activity.

the 100 kHz records (Fig. 5d). Pockmarks are also present and some are associated with seeps (Fig. 5e). The pockmarks are roughly circular and vary from 1–2 m across and up to 1 m deep to larger features 10 m across and 2 m deep. Sand waves (<1 m) occur between the reflective blocks, hard mounds and pockmarks, indicating sediment transport by waves and currents (Fig. 5f).

The variety of features, from well-defined pockmarks to reflective blocks arranged around the vent areas, seems to be related to the same process of seepage, but with a different degree of erosion. Water current and/or seepage erosion have probably modified the shape and size of the seabed features related to seepage, exposing the carbonate-cemented sediments. In Cornea areas 1 and 2 (Fig. 6a,b), clusters of reflective blocks are the most common feature in Cornea area 2, with more pockmarks in Cornea area 1. Above the Cornea oil and gas field, clusters of reflective blocks, larger hard-grounds and some pockmarks are clearly visible on the seafloor. In Cornea area 2 (Fig. 6b), more hard-grounds and mounds are observed.

In the North Sea, the conjunction of highly reflective seabed with shallow gas has been regarded as evidence of methane-derived authigenic carbonate (MDAC) (Judd, 2001). Similarly, in the Gulf of Mexico, strong seabed signal reflections were correlated to near-seafloor sediments with hard-grounds or crusts associated with hydrocarbon seep evolution (Sager et al., 2003; Sager et al., 2004).

In Cornea area 4, active seepage was not observed but the side-scan data imaged pockmark fields (identified previously by O'Brien et al., 2002a) and small mounds (up to 3 m high) between NW–SE trending channels and narrow hard-grounds (Fig. 7a). The process responsible for these pockmarks must have been active since the Holocene transgression, and be sufficiently active today to maintain their morphology against reworking by tidal currents, storm activity and cyclones (K. Glenn, pers. comm., 2004). The channels have high reflectivity shoulders on the side-scan sonar (Fig. 7b), suggesting that the channel margins are well lithified and resistant to erosion, but have a thin lag of sediment in the middle. These channels are aligned with the NNW–SSE tidal current direction in this region (Jones et al., 2005a) and also with the regional bathymetric slope. Thick Quaternary sediment accumulations have not been observed (Glenn, 2004), suggesting a lack of sediment supply onto the shelf and/or movement of sediment off the shelf.

4.2.2. Multi-beam bathymetry

The multi-beam bathymetry identified numerous features including some observed previously on 3D seismic data that were not resolved on hydrographic charts (Figs. 7 and 8). The features include: relatively small rises or hollows, less than 100 m across, relatively large mounds and palaeo-drainage channels likely to be associated with the Last Glacial Maximum. The resolution of the multi-beam bathymetry (around 5 m) was close to the diameter of pockmarks, and of small clusters of reflective blocks identified on the side-scan sonar, so it did not allow identification of fine-scale seabed features associated with seepage observed in Cornea areas 1 and 2. However, individual hard mounds and pockmark fields are usually located over subtle rises of less than 1 m high, or occasionally over mounds 3–6 m high (Fig. 8). Over Cornea area 2, a large 6 m high mound (82–88 m water depth), trending northwest, 1.6 km long and 0.7 km wide, is surrounded by low relief channels (Fig. 8). Active seeps have been observed on the eastern and northeastern side of this mound and are correlated with small-scale bathymetric rises (half a metre high). The elliptical shape of the 6 m high hard carbonate mound, was probably shaped by the strong NW–SE tidal current observed in the area. We interpret the mound as

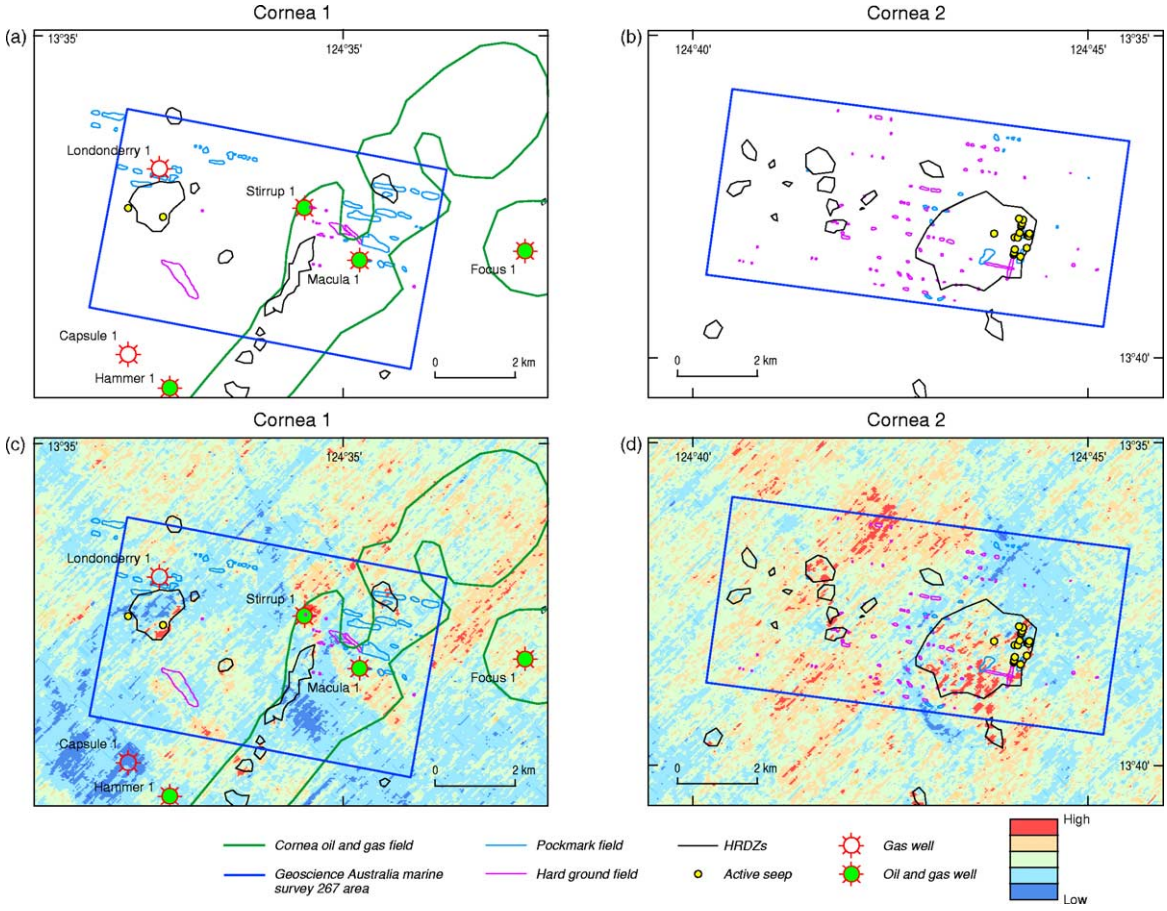

Fig. 6. Distribution of seabed features related to seepage compared to active seeps and HRDZs locations in the surveyed areas 1 and 2 (a,b). The same features are also correlated to the amplitude of the seafloor reflector interpreted from the Cornea 3D seismic data in the same areas 1 and 2 (c,d). The Cornea oil and gas field is located in Cornea area 1.

a surface expression of an HRDZ, formed by increased carbonate cementation caused by the oxidation of seeping methane.

Over Cornea areas 2 and 4, some pockmarks and small clusters of reflective blocks are found on the edge of channels. These channels are up to 3 m deep in Cornea area 2, up to 11 m deep over Cornea area 4, and up to 20 m deep further east of Cornea area 4. These channels have been shown to influence surface water flows, even in areas up to 80 m deep (Jones et al., 2005a). This influence has been observed in SAR studies which identify areas of flattened sea surface ('slicks') and was also observed from the survey vessel. Jones et al. (2005a)) demonstrated that the multibeam data are invaluable ground-truth SAR anomalies previously interpreted as oil slicks in the region.

4.2.3. Seabed sedimentology

4.2.3.1. At seeps. Close to seep areas (0–60 m distance), dredge and grab samples (Fig. 8) included coarse fractions composed of thick black cemented crust, mud pellets, Sabelariid worm tubes (some of which were covered with black encrusted material), coral fragments, shells and shell fragments (bryozoan, echinoids), but only minor living biota (Carsten Wolff, Australian Institute of Marine Science, pers. comm. 2004). A high proportion of the specimens are quite small (<1 cm) and relict. It is uncertain whether the sediment size is an artefact of the collection method, or representative of the seepage site. Several samples taken directly from seeps included small dark greyish carbonate blocks, some of which had a very strong smell of H_2S and contained particularly abundant dark encrusted material. The strong smell of H_2S indicates that sulphate reduction is active very close to the sediment–water interface at active seep sites, and is most likely associated with anaerobic methane oxidation.

4.2.3.2. Away from seeps. Grabs and dredges taken away from seepage areas also comprise bioclastic carbonate muddy sand, but with very little macro-biota or black encrusted material compared with seep site samples. The only intact shells are spinose gastropods, furthermore, Sabelariid worm tubes are absent. In Cornea area 2 (Fig. 8), above the centre of an HRDZ and away from the active seepage at the eastern edge, no coarse sediments were recovered during dredging and only minor shells or shell fragments were found, in contrast to abundant fauna/fragments at the active vent areas.

4.2.3.3. Carbonate mineralogy and isotope analysis. The light carbonates are aragonite of normal marine sediment origin,

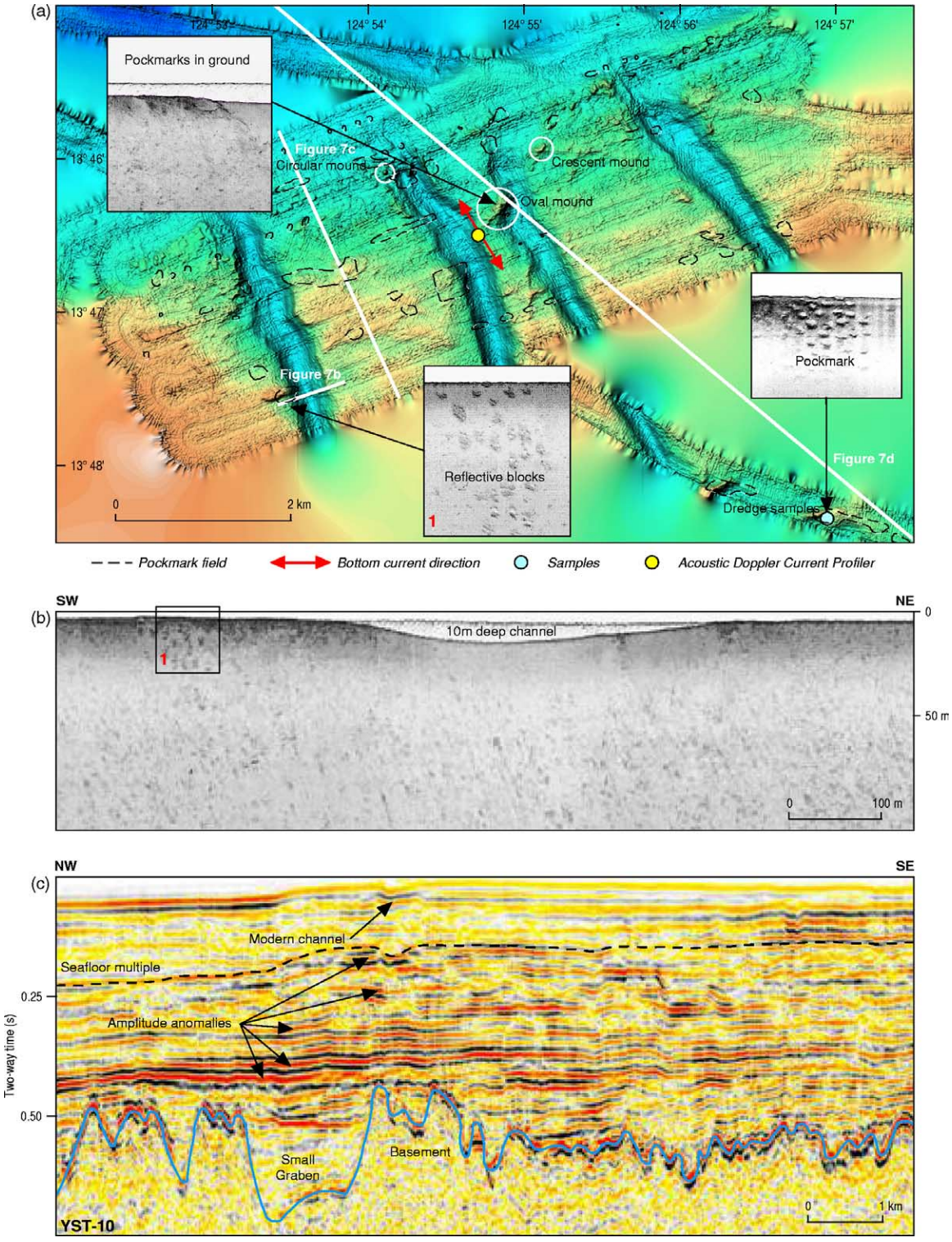

Fig. 7. (a) Shaded multibeam bathymetry over Cornea area 4 revealing four eleven-metre deep channels aligned with the NW–SE tidal current direction in this area (indicated by the arrow centred on the acoustic Doppler current profiler location represented by a yellow dot). In between the channels, 2–4 m high mounds are observed with oval, circular or crescent shapes. (b) Pockmark fields are observed on the levees of these channels. (c) 2D seismic line YST-10 showing structure beneath one channel. Seismic discontinuities and amplitude anomalies occur under the channel and above the basement highs.

whereas the greyish and dark encrusted materials are rhodochrosite ($MnCO_3$) which may be secondary carbonate related to seepage. However, the carbonate isotope analyses did not reveal any evidence of a hydrocarbon related origin. The carbon-13 and oxygen-18 isotope values were $\delta^{13}C$ −1.3–1.9‰ vs PDB and $\delta^{18}O$ 27.3–29.7‰ vs SMOW, indicating that the source of the bulk of the carbonate is from sea water bicarbonate. In contrast, hydrocarbon-derived carbonates have

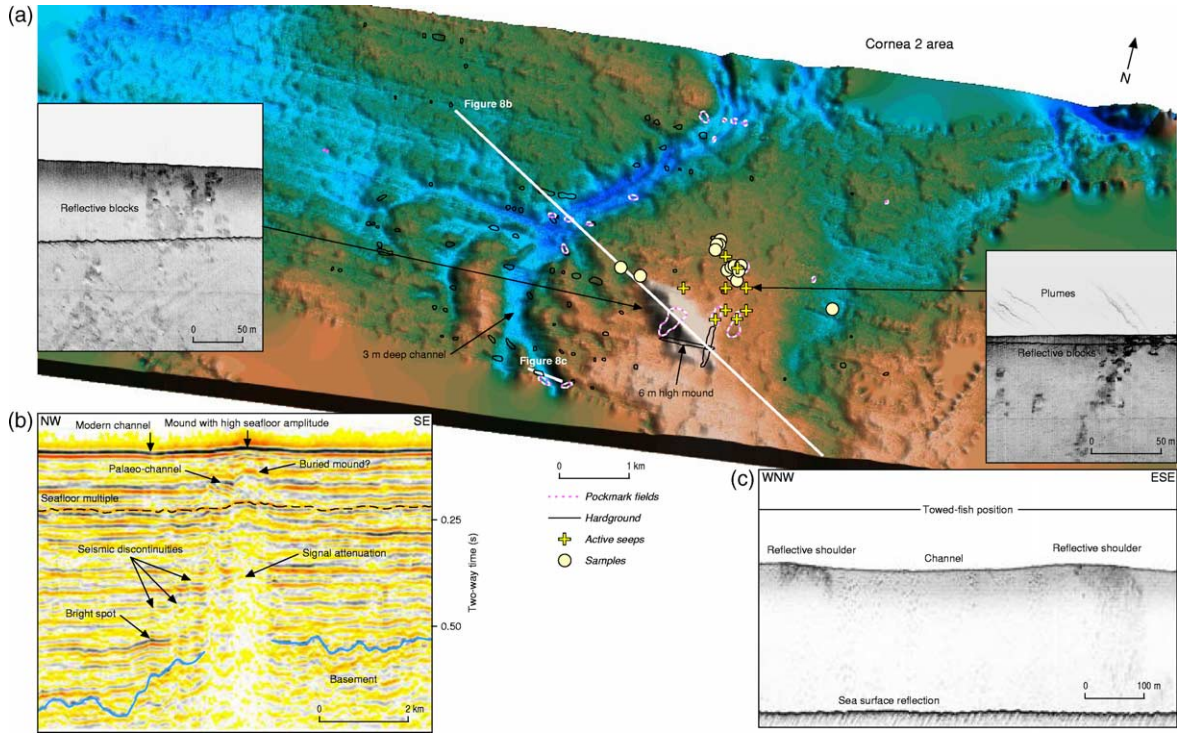

Fig. 8. (a) Shaded multibeam bathymetry over Cornea area 2 revealing a six-metre high mound surrounded by a three-metre deep channel and other features. (b) 3D seismic section showing the sub-surface features coinciding with the six-metre high mound on the seabed. (c) Side-scan sonar data across the three metre deep channel.

a distinctively light carbon-13 signature, unlike the carbonates analysed in this study. These results suggest that the geochemical signal of MDAC on an active tropical carbonate shelf may be swamped by abundant marine carbonates. This may be an important distinction in characterising MDAC in carbonate vs siliciclastic environments.

4.2.4. Subsurface features

2D and 3D seismic data were used to detect depressions and bumps on the seabed reflector, which were correlated with pockmarks and small encrusted mounds observed on the side-scan sonar imagery. Amplitude anomalies and interpreted HRDZs could also be detected in the 2D seismic data but were much better defined in the 3D data. The 3D data provide better coverage to image subtle features related to seepage.

4.2.5. Zones of seismic signal starvation and pull-up

In the 2D and 3D seismic data, acoustic layering is well-developed on the Yampi Shelf with no major fault disruptions. On the 3D seismic data, sub-circular high amplitude features with underlying attenuated seismic signal, or high velocity pull-up on the edges are probably related to cementation associated with HRDZs (Shell Development (Australia) Pty. Ltd., 2000). Numerous zones of acoustic signal attenuation are observed over Cornea areas 1 and 2, with abrupt lateral and vertical terminations (Fig. 9). In many cases the seafloor horizon exhibits high amplitudes above the interpreted HRDZs, and all of the observed active seeps are located on the edge of seafloor high amplitude zones (Figs. 8 and 9).

Based on our field observations and seismic analysis we support the interpretation of the sub-circular high amplitude features with attenuated seismic signal or pull-up on all horizons as HRDZs, but there is no carbonate isotope data to confirm this interpretation.

On the seismic cross-section from Cornea area 2 (Fig. 9b), small-scale undulations on the seabed reflector and above HRDZs are correlated with plumes in the water column, small clusters of reflective blocks, hard-grounds and pockmarks in the side-scan sonar data. In the subsurface, a zone of disturbed seismic facies (Figs. 8b and 9b) occurs under the 6 m high mound observed on the seabed (Fig. 8a).

This zone is characterised by the following features (described from NW to SE on Fig. 8b):

(1) A bright spot is observed in a horizon draping a basement high, and could represent a gas pocket.
(2) Small-scale seismic discontinuities with pull-ups on the sides suggest either the presence of local HRDZs and/or micro-discontinuities in the sediments, associated with vertical hydrocarbon migration through the sediment layers.
(3) A zone of seismic signal attenuation associated with possible HRDZs present in the shallow sediment layers (high amplitude reflectors between 160 ms TWT and the seafloor), a probable buried mound or HRDZ and a 6 m high mound on the seabed, both with a high seafloor amplitude.

In the eastern part of Cornea area 1, pockmarks and clusters of reflective blocks lie north of the NE–SW elongate HRDZ, above the known oil and gas field area (Fig. 6a). Thus, seepage

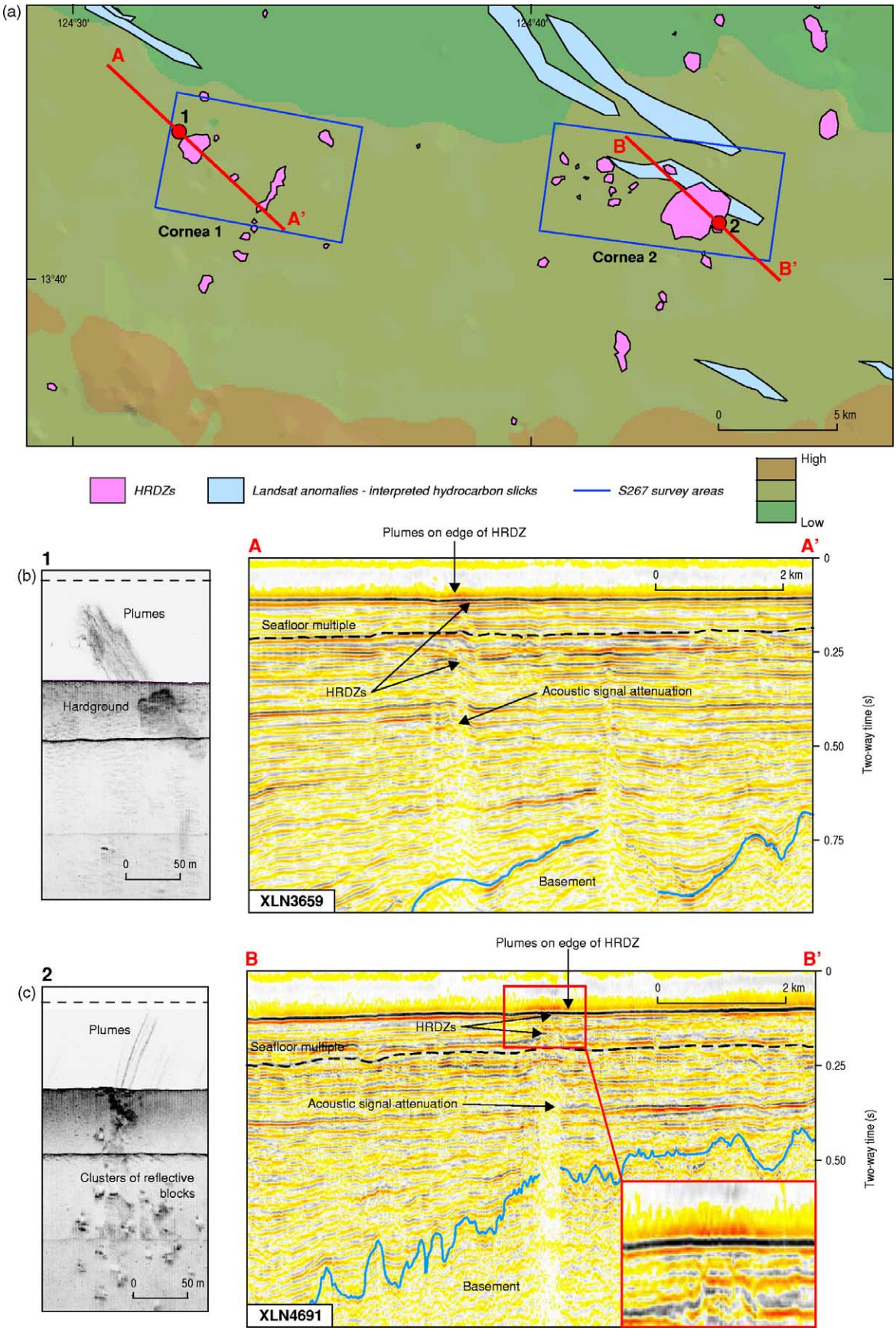

Fig. 9. 3D seismic sections illustrating HRDZs and other features near active seep sites in Cornea areas 1 and 2. (a) Map shows location of two seismic sections A-A′ and B-B′ which run over active seep locations and HRDZs. (b) Side-scan sonar image of active gas seepage at location 1. (c) Side-scan sonar image of active gas seepage at location 2.

is interpreted to occur above the oil and gas accumulation, but was not observed during the survey. However, the present location of hard-grounds and pockmark fields does not always correspond with the location of HRDZs. This suggests that hydrocarbon migration pathways to the seafloor may have shifted over time (Hovland, 2002).

4.2.6. Seismic amplitude

The correlation between the amplitude of the seafloor reflector and the location of seabed features imaged by side-scan sonar data over Cornea areas 1 and 2 (Fig. 6c,d) demonstrates that high amplitudes correspond with hard-grounds, clusters of reflective blocks or rough surfaces. Conversely, low amplitudes appear to correlate with soft sediments and channels.

In some cases, the highest seafloor amplitudes are centred above buried HRDZs, as in Cornea area 2 (Fig. 6d). This suggests that this particular HRDZ has been active for a long period of time. This is supported by the existence of a 6 m high mound observed on the seafloor above a buried mound and/or HRDZ (Fig. 8, at 160 ms TWT). In Cornea areas 1 and 2, the presence of active seeps on the edge of HRDZs suggests that the present-day migration pathway to the seabed has been impeded by the development of a carbonate cemented 'cap' above the seep conduit. Such correlation between seepage and seafloor mounds and high backscatter has also been observed on the upper continental slope of the northern Gulf of Mexico (Roberts, 2001; Sager et al., 1999, 2004).

The seafloor reflector is commonly of low amplitude around the margins of the HRDZs, where channels are visible on multi-beam bathymetry (Fig. 7a and 8a), and where side-scan data show very shallow depressions on the seabed (Fig. 7b and 8c). The different reflectivity observed on the side-scan sonar data between the centre and the shoulders of the channels reveals that the shoulders are cemented compared to the soft sediments which are probably mobile bed load in the axis of the channels.

4.3. Relation between seeps and tidal cycles

Observation of variable seepage rate at the same locations at Cornea areas 1 and 2 during different times of the tidal cycles indicates that there is a direct correlation between the tide height and the rate of seepage. The North West Shelf is known as one of the largest macro-tidal shelf environment (Harris, 1994) and the tidal difference on the Yampi Shelf can be up to 5 m during the spring tide (Flinders Institute for Atmospheric and Marine Sciences, 1997; Flater and Pentcheff, 2004). Active seepage was observed both on side-scan and echo-sounder data during low tide and most strongly on the ebb tide, less than two hours before low tide. During ebb tides, the height of the water column decreases several metres (~5–10%) and the consequent reduction in total water pressure generates a difference of interstitial pore pressure allowing the expulsion of gas from the sediments into the water column forming plumes. In Fig. 10, side-scan sonar images are from the same area but at different times of the

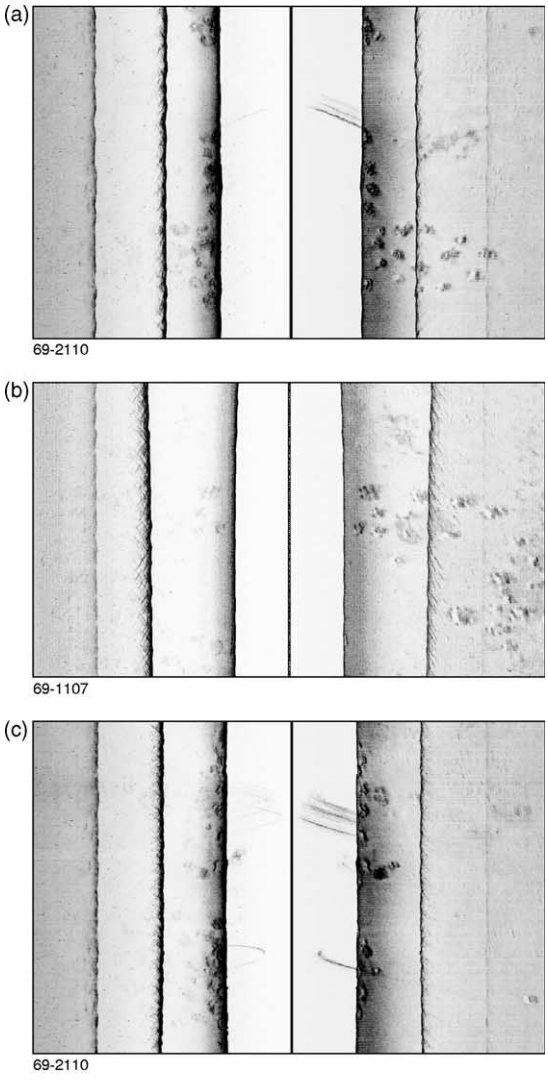

No -IV-	UTC Details	UTC Time	Tide	Tide Height (m)	Day/ Night	Turn of Tide
a)	9/03/04	21:20	Ebb	0.66	N	1 hour
b)	9/03/04	11:54	Flood	0.81	D	1 and a half hours
c)	9/03/04	21:54	Ebb	0.35	N	30 minutes

Fig. 10. Side-scan sonar data imaging gas plumes in the water column at different phases of the tidal cycle (situated approximately at the same location in Cornea area 2. (a) and (c) show gas plumes during ebb tide, while (b) shows no plume during flood tide.

semi-diurnal tidal cycle. Images recorded on ebb tide (Fig. 10a,c), show gas plumes in the water column above clusters of reflective blocks on the seabed. Fig. 10b shows the same cluster of reflective blocks one and a half hours after low tide, but no plumes were observed in the water column during this flood tide. Plumes were also more active during the low spring tidal cycles (5 m tides) compared to low neep tides (2 m tides). Above the Coal Oil Point seep field in California, strong evidence for temporal variability in seepage rates is also observed, responding to diurnal tidal forcing and

a longer period (a few months) of unknown origin (Boles et al., 2001; Leifer, 2003; Clark, 2004).

Elsewhere in the world, correlation between seepage and tidal cycles (see above), earthquakes (Hasiotis et al., 1996), storms or rig/platform emplacements (Judd, 2001), shows that seepage can be triggered by a variety of external events. Although tropical cyclones Evan and Fay cut short the survey program on the Yampi Shelf, the effects of these cyclonic low atmospheric pressures, immediately before and after the survey, respectively, may have contributed to seep behaviours.

These observations suggest that if hydrocarbon migration pathways exist on the shelf, seepage could be more easily triggered on the upper and middle shelf (less than 100 m water depth) where the macro-tidal influence and tropical cyclones have their biggest effect.

4.4. Possible relict seepage features over Cornea area 4

Although no active seepage was observed in Cornea area 4, 35 km E-SE of the Cornea oil and gas field, some evidence of recent seepage is inferred by the presence of pockmark fields (O'Brien et al., 2002a; this study) and hard-grounds between 11 m deep channels. These channels show closed bathymetric contours (Fig. 7a) and are located on a palaeo-headland between a palaeo-shallow lagoon inboard and a deeper mid-shelf outboard (Jones et al., 2005a). Their shape and location suggest that they may have been formed at a sea-level lowstand by tidal current flow within inlets between barrier islands (Jones et al., 2005a). The presence of sand-waves immediately adjacent to the channel margins, and crescent-shaped mounds between 58 and 60 m depth (Fig. 7a), indicate that strong near-bed currents are still active. Also a strong near-bed tidal current ($\sim$1.5 knots) was recorded in one of these channels over Cornea area 4 on an Acoustic Doppler Current Profiler (ADCP) deployed during the survey (Fig. 7a) (Jones et al., 2005a).

Numerous 2–4 m high mounds are observed between the tidal-scour channels (Fig. 7a). The larger ones have an oval shape and are about 150–300 m long and 30–60 m wide. A series of smaller circular mounds (30 m in diameter; Fig. 7a), have also been mapped by the multi-beam bathymetry on the flanks of the four 11 m-deep-channels aligned with tidal flow along the bathymetric headland. Pockmark fields are observed either on the top or on the side of these mounds. The mounds appear to coalesce to form a 2–3 m high terrace (at 56–57 m depth) that presumably records a previous sea-level lowstand (Fig. 7c).

The origin of these mounds and pockmarks is not certain. Dredge samples from the two southernmost pockmark fields (Fig. 7a) are associated with two elongated mounds ($>$300 m long and 3 m high) and coral fragments covered by a coralline algae crust which includes bivalves, small serpulid worm tubes ($<$1 mm in diameter), bryozoans, foraminifera, pteropods and heteropods. These dredge recoveries do not include Sabelariid worm tubes, dark coloured encrusted materials or any smell of H_2S, like those recovered from present-day active seep sites, in Cornea areas 1 and 2. Because of the lack of direct evidence for seepage in Cornea area 4, we cannot exclude the possibility that the features in this area may be formed through karst processes during sea level lowstand.

However, it appears from a correlation with the subsurface that the tidal scours coincide with basement highs (Fig. 7d). Seismic discontinuities and high amplitude reflectors are also observed beneath these channels, suggesting possible leakage and the presence of hydrocarbons in the underlying section (Fig. 7d). Although active seepage was not observed in this area, even at low tide, the presence of pockmark fields and hard-grounds on the margins of the tidal scours suggests that fluid has recently escaped to the seafloor.

4.5. Summary of seepage features

The various geophysical techniques used during this survey show different seepage-related features depending on the scale or degree of resolution and nature of the data (Table 2):

1. Echo-sounder data revealed plumes of bubbles in the water column from the seafloor, which are direct evidence of seepage. These rarely reached the sea surface, instead being trapped in a layer at 40–60 m depth. This layer is possibly an iso-density surface, or an oceanic methane layer formed when particles lifted by bubbles are abandoned when the bubbles dissolve (Leifer and Judd, 2002).
2. Side-scan sonar data also show these plumes in the water column, and features on the seabed from which they emanate. These features include clusters of reflective blocks, hard-grounds, mounds and small pockmarks.

Table 2
Range of scale and relevance of the various geophysical data used during this study for seepage detection and characterisation

Equipment type	Scale	Relevance/application
Echo-sounder (200 kHz)	Image the water column with $<$50 cm resolution	Essential for seep detection, visualisation of gas plumes in the water column. Very useful tool for positioning ship over the vents
Side-scan sonar (100 and 500 kHz)	Image the water column and the seabed with different backscatters with $<$1 m resolution	Essential for seep detection and mapping geo-referenced locations of related seabed features
Multi-beam bathymetry (180 kHz)	Image the seabed with approximately 5 m resolution	Important for integrating the small scale hydrocarbon-related features with the surrounding environment
Seismic 2D	Image the seabed and underlying layers with 12.5 m resolution along the line	Important for correlating seabed features related to seepage with underlying geology and hydrocarbon migration pathways
Seismic 3D	Image the seabed and underlying layers with 12.5 m resolution in 3D	Important for correlating high resolution seabed features related to seepage with underlying geology and hydrocarbon migration pathways. Also important to get total 3D view of features and not just a cross-section

3. Multi-beam bathymetry data identified small-scale rises, between 0.5 and 3 m high, in close proximity to seepage areas. Encrusted carbonate mounds are found above long-lived HRDZs, such as the 6 m high mound observed in Cornea 2 study area. Erosion around them and/or active carbonate precipitation due to methane derived authigenic carbonate may have enhanced their morphology.
4. Sediment samples indicate a more diverse biota, including abundant Sabelariid worm tubes, and greater cementation at, and near, seeps than in non-seep areas.
5. Seismic data, especially the 3D dataset, indicate HRDZs on the seabed and in the shallow sediment layers. These data also show undulations on the seabed above HRDZs that correlate with clusters of reflective blocks, hard-grounds and pockmark fields.
6. Seepage activity is directly controlled by tidal cycles and is most active at low ebb tides.

5. Regional correlation of seepage features

5.1. Aeromagnetic anomalies

Aeromagnetic data were acquired in 1996, by World Geoscience Corporation Ltd, along 400 m-spaced N–S traverse lines and 1200 m-spaced E–W tie lines, with a survey flying height of 80 m (Nash and Belford, 1996). Magnetic anomalies reveal prominent lineations (1–2 km wide and 80–100 km long) along two perpendicular trends, NW–SE and NE–SW (Fig. 11). The depth of these magnetic anomalies, between 500 and 800 m (M. Morse, Geoscience Australia, pers. comm., 2004), indicates that the lineations are related to basement structures. Regional lineaments, on the North West Shelf, with similar trends, were also identified as corridors approximately 100 km in width and often exceeding 1000 km in length (Elliott et al., 1996). Active seepage in Cornea area 1 is located along the NE trending positive magnetic anomalies, whereas active seepage in Cornea area 2 is located close to where the NW trending positive magnetic anomalies are off-set and cross-cut by the conjugate NE trending positive magnetic anomalies (Fig. 11). Comparison of these magnetic lineations with the seismic, bathymetry, side-scan sonar and echo-sounder data indicates that areas of active seepage and seafloor channels occur along the magnetic lineations and close to their orthogonal intersections.

Tertiary fault activity is not apparent on seismic data on the Yampi Shelf, but faults may be present with throws less than seismic resolution [approximately 10 m; Shell Development (Australia) Pty. Ltd., 2000]. However, within the basement, a conjugate Proterozoic dyke-filled fracture system extends out from the onshore Kimberley Block (Etheridge and Wall, 1994; O'Brien et al., 1996). These fracture systems have controlled present-day topography in the onshore Kimberley Ranges (Gunn and Meixner, 1998). They are imaged as a conjugate

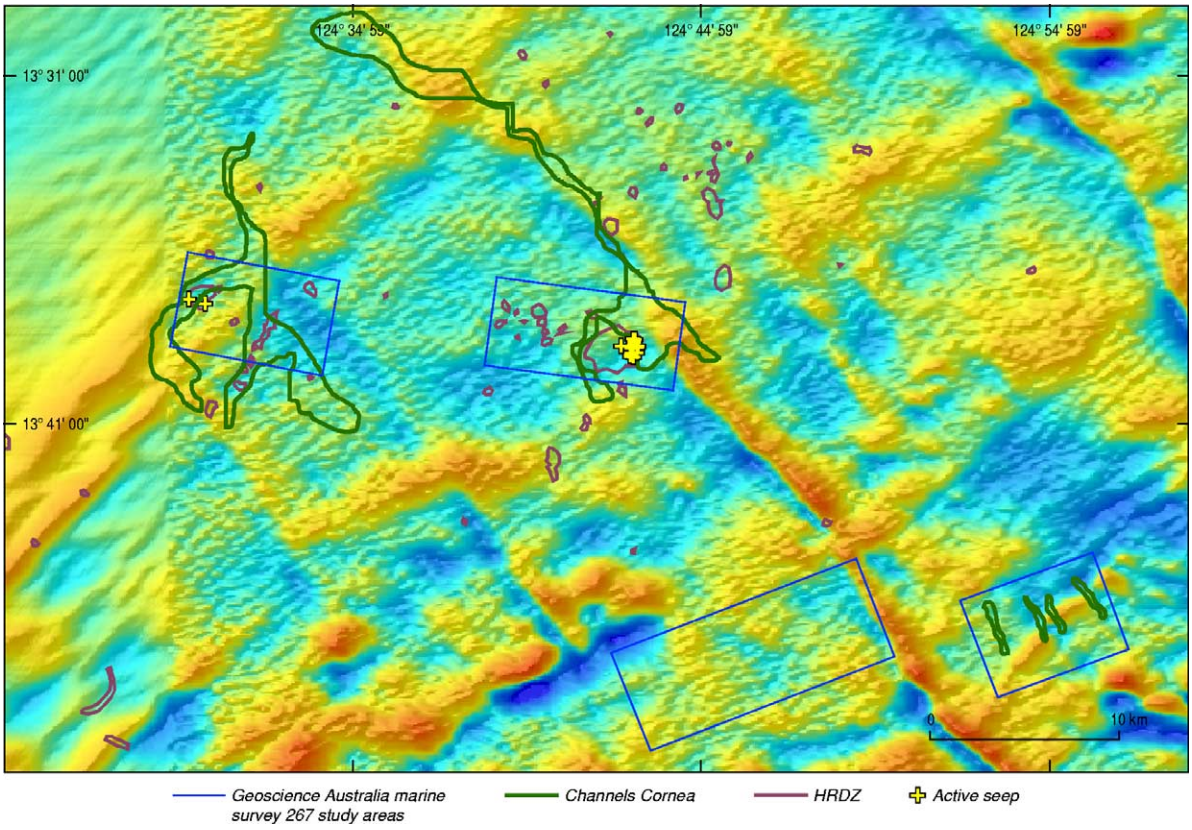

Fig. 11. Aeromagnetic anomaly grid of the first vertical derivative reduced to the pole shows magnetic lineations over the study areas. Lower resolution data are on the western side of the map. Active seepage and related features (pockmarks, clusters of hard blocks and hard-grounds) are preferentially located in areas where the NW trending positive magnetic anomalies are off-set and cross-cut by the conjugate NE trending magnetic anomalies.

series of linear magnetic anomalies onshore (Gunn et al., 1995), and are also interpreted to extend offshore to the Yampi Shelf (O'Brien et al., 1996), including the present survey area (Cornea areas 1, 2, 3 and 4). Active seepage is observed in this area where the NW trending positive magnetic anomalies, interpreted as fractures in-filled with dolerite dykes, are off-set and cross-cut by the conjugate NE trending positive magnetic anomalies (Fig. 11).

5.2. Structural control on seepage

Focussed fluid migration along faults, discontinuities or unconformities is much more effective than non-focussed seepage through a sedimentary column (Abrams, 1992; Brown, 2000).

Along the North West Shelf, NE–SW extensional faults have been reactivated several times since the early Triassic, especially during the Late Miocene–Early Pliocene convergence of the Australian and Eurasian plates (O'Brien et al., 1999b; Keep and Moss, 2000; Keep et al., 2002). The pre-existing, conjugate dyke-filled fracture system in the basement rocks may also have been reactivated at this time. A second mechanism that may have initiated leakage and fracture/fault reactivation was basin tilting in the Miocene. This resulted in the tilting of traps along the eastern Browse Basin margin, causing oil to remigrate and spill updip (Keall and Smith, 2000). The oil that migrated into traps around the Gwydion and Cornea fields during the Miocene could be currently seeping following more recent reactivation of fracture zones. A third and more subtle mechanism that may have caused reactivation of pre-existing fractures was the rebound after tilting of the continental margin caused by the Holocene sea-level rise (Nakada and Lambeck, 1989).

At the Skua oil field in the Timor Sea, 126 km north of the study area, fault intersections have been identified as efficient and long-lived fluid conduits (Cowley and O'Brien, 2000; Gartrell et al., 2002, 2003, 2004). A similar scenario could be applicable to Cornea areas 1 and 2, where both present-day (gas plumes) and palaeo-seepage HRDZs indicators are observed above fracture intersections in the basement. Fluids other than hydrocarbons could also benefit from these micro-fracturing pathways to the seafloor. The Cornea oil accumulation is heavily biodegraded (Boreham et al., 1997; Blevin et al., 1998; Edwards et al., 2003), and thus meteoric fluids moving along these basement fractures could have been one mechanism for the biodegradation of the Cornea oils.

5.3. Palaeo- and present-day channels

On the Yampi Shelf, present-day channels are observed on the seabed on the multi-beam bathymetry data (Figs. 7 and 8), and numerous palaeo-channels are also observed in the Pliocene/Pleistocene in the 3D seismic data (typically between 180 and 250 ms TWT depth; Fig. 12). These present-day and palaeo-channels are orientated perpendicular to the shelf, parallel to the tidal current and also parallel to the NW set of magnetic lineaments (Fig. 10). Active seeps and seepage related features (cemented mounds and pockmarks) are mainly located on the edges of these modern channels or above the margins of Pliocene/Pleistocene palaeo-channels (Figs. 7 and 8). In the channels on the shelf, the sediment type changes away from their banks. The channel bottom mostly consists of low backscatter bioclastic and maybe siliciclastic sediments and could act as local fluid reservoirs. The close spatial association of seeps to subsurface and seabed channels suggests that these channels may be acting as conduits for migrating, shallow gas. Major lineaments related to dykes/faults may also provide horizontal conduits for seeping fluids in Cornea areas 1 and 2, as suggested by the relationship with active seeps, seabed related features and channels (as discussed in Section 5.2). In Cornea area 4, the nature of the fluid is not proven. However, the potential hydrocarbon migration pathway is along permeable conglomeratic layers sitting on the basement. In this scenario, seepage above basement highs could occur and be modified by the shallow channels so that channel edges become sites of sea floor seepage.

Palaeo-channels recorded on the lower slope of the Congo Basin, West African margin, provide preferential conduits for horizontal hydrocarbon migration and can trigger vertical leakage at an early stage of their burial history (sediment cover thickness between 130 and 240 m; Gay et al., 2003). The burial of channels induces a fluid flow caused by a longitudinal pressure gradient along the palaeo-channel. The resulting pressure of hydrocarbon migration from deeper over-pressured reservoirs could contribute to the pore fluid pressure in the shallow subsurface sediments. Therefore, seepage is enhanced over channels where fluids are trapped at intermediate reservoirs (Gay et al., 2003).

6. Preservation and characterisation of seepage features on the Yampi tropical macro-tidal carbonate shelf

The detection and differentiation of present-day seepage vs palaeo-seepage are particularly difficult on a tropical carbonate shelf where the overall modern sedimentation rate is low, resulting in a veneer of mixed old and new sandy carbonate sediments and indurated seabed features.

Seepage related features on the Yampi Shelf are mostly small (reflective blocks, hard-grounds, mounds and pockmarks, <10 m in diameter and less than 10 m high or deep). These features are located mainly on the upper and middle shelf in warm water (23–28 °C; James et al., 2004) where the sedimentation is storm-dominated and where macro-tidal fluctuations have significant impact on sediment movement. High-energy conditions prevail along the whole North West Shelf where sediments are strongly mixed and eroded by the action of strong internal tides, between approximately 50 and 100 m water depth (James et al., 2004). Furthermore, sea-level changes have modified the shelf morphology and sedimentology. Large-scale seepage features (e.g. big pockmarks) are unlikely to form in these sandy sediments, and smaller scale seepage features (small pockmarks) are unlikely to be preserved unless the seepage is active today.

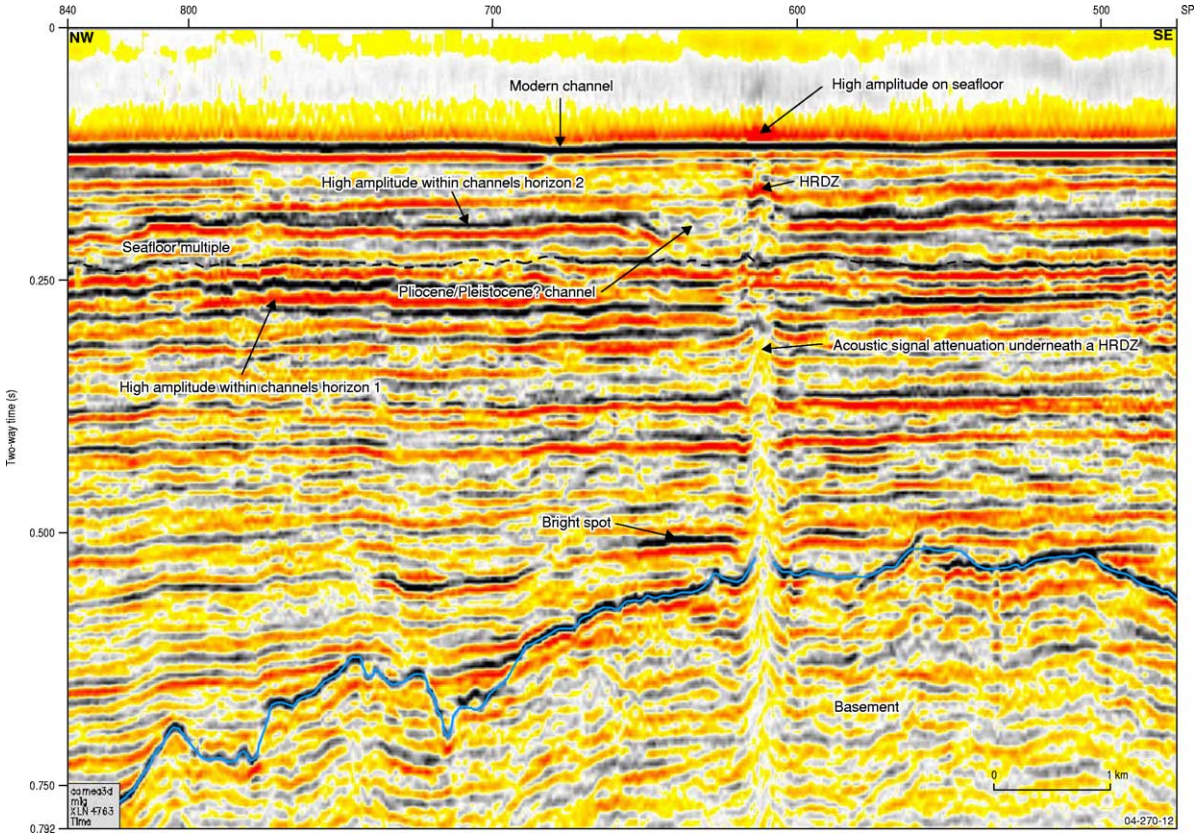

Fig. 12. 3D seismic section showing the development of a palaeo-channel (Plio-Pleistocene?) on the edge of a HRDZ in Cornea area 2. The high amplitude on the seafloor causes acoustic signal attenuation underneath and is located directly above a basement high. Micro-fracturing is also observed from the top of the basement and into the above sedimentary layers.

The small size of the seepage related features may also relate to the tectonic stress regime on the North West Shelf. Typically large seepage features develop in compressional settings (Table 1). Although the Yampi Shelf did have some compressional reactivation, the change in tectonic setting at this location on the North West Shelf from a passive to a collisional margin did not allow the establishment of a strong compressional stress regime where large seepage-related features would be generally observed (Table 1). The main compression is located along the Timor Trough, approximately 300 km north of the Yampi Shelf. Therefore, the Yampi Shelf has a fluid migration regime more like a passive margin.

7. Conclusion

Active hydrocarbon seepage has been observed and characterised on the Yampi Shelf using a range of data, which provide different levels of resolution. The echo-sounder and side-scan sonar data were essential for the detection of active seepage in the water column and to observe the seepage activity, which appears to be strongly influenced by pressure changes associated with macro-tidal cycles, and possibly atmospheric cyclonic lows. Side-scan sonar data identified specific seabed features at active plume vents (clusters of reflective blocks, hard-grounds, and pockmark fields). Multibeam bathymetry data identified small-scale rises (0.5–3 m high) in close proximity to seepage areas. Larger encrusted mounds are found above long-lived hydrocarbon-related diagenetic zones (HRDZs). Erosion around these mounds and/or active build-up from the seafloor may have enhanced their morphology. Correlation with 2D and 3D seismic profiles allows the identification of seepage features within the subsurface stratigraphic section (modern and palaeo-HRDZs, channels, seismic discontinuities and bright spots).

The integration of these datasets with aeromagnetic data helped to identify potential migration-seepage pathways. Magnetic anomalies reveal lineations related to basement structures, fracture zones and dykes. These structures can be correlated to areas of active seepage and palaeo- and modern channels on the seabed. The close spatial relationship of reactivated basement fractures and palaeo- and modern channels appears to have generated migration pathways for hydrocarbon seepage on the Yampi Shelf.

A significant characteristic of seepage features on the tropical carbonate Yampi Shelf is their small scale (<10 m in diameter and less than 10 m high or deep) compared to seepage features observed in siliciclastic and/or deeper water environments. The coarse-grained carbonate sediments and high-energy macro-tidal environment on this shaved shelf prevent the formation and preservation of larger scale seepage features.

Acknowledgements

The authors wish to thank Jon Stratton, Craig Wintle and Jack Pittar for their valuable technical assistance provided during Geoscience Australia marine survey 267. Mark Winters (skipper) and the crew of the *Parmelia K* also provided invaluable support during the survey. Special appreciation is extended to Kriton Glenn, Michael Abrams and Alan Judd for valuable discussions, Anne Fleming for her 3D seismic technical support, Andrew Barrett for generating the amplitude extraction of the seafloor reflector from the Cornea 3D seismic data, and Michael Morse for the magnetic anomaly processing. We also thank Andrew Barrett, Heike Struckmeyer, Jim Colwell, Andrew Heap, Martin Hovland and an anonymous reviewer for their constructive input to the manuscript. This paper is published with the permission of the Chief Executive Officer, Geoscience Australia.

References

Abrams, M., 1992. Geophysical and geochemical evidence for subsurface hydrocarbon leakage in the Bering Sea, Alaska. Marine and Petroleum Geology 9, 208–221.

Abrams, M.A., Segall, M.P., 2001. Best practices for detecting, identifying and characterizing near-surface migration of hydrocarbons within marine sediments. Offshore Technology Conference in Houston, Texas.

Bishop, D.J., O'Brien, G.W., 1998. A multi-disciplinary approach to definition and characterisation of carbonate shoals, shallow gas accumulations and related complex near-surface sedimentary structures in the Timor Sea. APPEA Journal 38 (1), 93–113.

Blevin, J.E., Boreham, C.J., Summons, R.E., Struckmeyer, H.I.M., Loutit, T.S., 1998. An effective lower cretaceous petroleum system on the North West Shelf: evidence from the Browse Basin. In: Purcell, P.G., Purcell, R.R. (Eds.), The Sedimentary Basins of Western Australia 2. Proceedings of PESA Symposium, Perth, pp. 397–419.

Boetius, A., Ravenschlag, K., Schubert, C.J., Rickert, D., Widdel, F., Gieseke, A., Amann, R., Jørgensen, B.B., Witte, U., Pfannkuche, O., 2000. A marine microbial consortium apparently mediating anaerobic oxidation of methane. Nature 407, 623–626.

Boles, J.R., Clark, J.F., Leifer, I., Washburn, L., 2001. Temporal variation in natural methane seep rate due to tides, coal oil point area, California. Journal of Geophysical Research 106, 27077–27086.

Boreham, C.J., Roksandic, Z., Hope, J.M., Summons, R.E., Murray, A.P., Blevin, J.E., Struckmeyer, H.I.M., 1997. Browse Basin organic geochemical study, North West Shelf, Australia. Interpretation Report, vol. 1, Australian Geological Survey Organisation, Record 1997/57.

Brown, A., 2000. Evaluation of possible gas microseepage mechanisms. AAPG Bulletin 84 (11), 1775–1789.

Casas, D., Ercilla, G., Baraza, J., 2003. Acoustic evidences of gas in the continental slope sediments of the Gulf of Cadiz (E Atlantic). Geo-Marine Letter 23, 300–310.

Christodoulou, D., Papatheodorou, G., Ferentinos, G., Masson, M., 2003. Active seepage in two contrasting pockmark fields in the Patras and Corinth gulfs, Greece. Geo-Marine Letter 23, 194–199.

Clark, J., 2004. Characteristics of Seepage at the Coal Oil Point Seep Field, Santa Barbara Channel, CA. Geoscience Australia Seminar, June 2004.

Cook, R., 2000. Mapping and characterising of natural hydrocarbon seepage in Australia's Timor Sea using Landsat TM data: a pilot project with AGSO Petroleum and Marine Division. Image Analysis & Mapping Pty Ltd report, March, 2000.

Cowley, R., O'Brien, G.W., 2000. Identification and interpretation of leaking hydrocarbons using seismic data: a comparative montage of examples from the major fields in Australia's North West Shelf and Gippsland Basin. APPEA Journal 40, 121–150.

Dando, P.R., Austen, M.C., Burke, R.J., Kendall, M.A., Kennicutt, M.C., Judd, A.G., Moore, D.C., O'Hara, S.C.M., Schmaljohann, R., Southward, A.J., 1991. Ecology of a North Sea pockmark with an active methane seep. Marine Ecology Progress Series 70, 49–63.

De Beukelaer, S.M., MacDonald, I.R., Guinnasso Jr., N.L., Murray, J.A., 2003. Distinct side-scan sonar, RADARSAT SAR, and acoustic profiler signatures of gas and oil seeps on the Gulf of Mexico slope. Geo-Marine Letter 23, 177–186.

Edwards, D.S., Crawford, N., 1999. UV fluorescence analysis of seawater samples from AGSO marine survey 207, Northwest Australia. Australian Geological Survey Organisation Record 1999/52, 7, unpublished.

Edwards, D.S., Preston, J.C., Kennard, J.M., van Aarssen, B.G.K., Boreham, C.J., Zumberge, J.E., 2003. Geochemical characteristics of hydrocarbon families and petroleum systems, Bonaparte Basin. Proceedings of the PESA and NT Department of Business, Industry and Resource Development, Timor Sea Symposium, Darwin, 2003.

Eichhubl, P., Greene, H.G., Naehr, T., Maher, N., 2000. Structural control of fluid flow: offshore fluid seepage in the Santa Barbara Basin, California. Journal of Geochemical Exploration 69–70, 545–549.

Elliott, C.I., Liu, S., Willcox, B., Petkovic, P., 1996. A lineament tectonic study of the basement architecture of Northwestern Australia, Australian Geological Survey Organisation Record No. 1996/50 1996.

Ergün, M., Dondurur, D., Cifçi, G., 2002. Acoustic evidence for shallow gas accumulations in the sediments of the Eastern Black Sea. Terra Nova 14, 313–320.

Etheridge, M., Wall, V.J., 1994. Tectonic and structural evolution of the Australian proterozoic. Geological Society of Australia 37, 102–103.

Etheridge, M., McQueen, H., Lambeck, K., 1991. The role of intraplate stress in Tertiary (and Mesozoic) deformation of the Australian continent and its margins: a key factor in petroleum trap formation. Exploration Geophysics 22, 123–128.

Flater, D., Pentcheff, D., 2004. WWW tide and current predictor, Biological Sciences. University of South Carolina, Columbia, USA.

Flinders Institute for Atmospheric and Marine Sciences, 1997. National Tide Facility. Flinders University of South Australia.

Fugro Airborne Surveys Pty Ltd, 2001. ARGUS Offshore Test Survey: Cornea-April 2001. Data Evaluation Report for AGSO, Petroleum, unpublished report.

Garcia-Garcia, A., Orange, D.L., Maher, N.M., Heffernan, A.S., Fortier, G.S., Malone, A., 2004. Geophysical evidence for gas geohazards off Iskenderun Bay, SE Turkey. Marine and Petroleum Geology 21, 1255–1264.

Gartrell, A., Lisk, M., Undershultz, J., 2002. Controls on the trap integrity of the Skua Oil Field, Timer Sea. In: Keep, M., Moss, S.J. (Eds.), The Sedimentary Basins of Western Australia 3. Proceedings of PESA Symposium, Perth, pp. 389–407.

Gartrell, A., Zhang, Y., Lisk, M., Dewhurst, D., 2003. Enhanced hydrocarbon leakage at fault intersections: an example from the Timor Sea, Northwest Shelf, Australia. Journal of Geochemical Exploration 78-79, 361–365.

Gartrell, A., Zhang, Y., Lisk, M., Dewhurst, D., 2004. Fault intersections as critical hydrocarbon leakage zones: integrated filed study and numerical modelling of an example from the Timor Sea, Australia. Marine and Petroleum Geology 21, 1165–1179.

Gay, A., Lopez, M., Cochonat, P., Sultan, N., Cauquil, E., Brigaud, F., 2003. Sinuous pockmark belt as indicator of a shallow buried turbiditic channel on the lower slope of the Congo basin. In: Van Rensbergen, P., Hillis, P., Maltan, A.J., Morley, C.K. (Eds.), Subsurface Sediment Mobilization. Geological Society, London, Special Publications, vol.216, pp. 173–189.

Glenn, K., 2004. Sedimentary processes during the Late Quaternary across the Kimberley Shelf Northwest Australian. University of Adelaide, unpublished PhD thesis.

Glenn, K., O'Brien, G.W., 2002. Coral reefs & hydrocarbon seeps. AusGeoNews, Geoscience Australia 68, 4–7.

Gunn, P.J., Meixner, A.J., 1998. The nature of the basement to the Kimberley Block, Northwestern Australia. Exploration Geophysics 29, 506–511.

Gunn, P.J., Brodie, R.C., Mackey, T., O'Brien, G.W., 1995. Evolution and structuring of the Joseph Bonaparte Gulf as delineated by aeromagnetic data. Exploration Geophysics 26, 255–261.

Harris, P.T., 1994. Comparison of tropical, carbonate and temperate, siliciclastic tidally dominated sedimentary deposits: examples from the Australian continental shelf. Australian Journal of Earth Science 41, 241–254.

Hasiotis, T., Papatheodorou, G., Kastanos, N., Ferentinos, G., 1996. A pockmark field in the Patras Gulf (Greece) and its activation during the 14/7/93 seismic event. Marine Geology 130, 333–344.

Heyward, A., Pinceratto, E., Smith, L., 1997. Big bank shoals of the Timor Sea: an environmental resource atlas, Australian Institute of Marine Science, BHP Petroleum 1997. 115 pp.

Hovland, M., 1990. Do carbonate reefs form due to fluid seepage? Terra Nova 2, 8–18.

Hovland, M., 2002. On the self-sealing nature of marine seeps. Continental Shelf Reseach 22, 2387–2394.

Hovland, M., Judd, A.G., 1988. Seabed pockmarks and seepages: impact on geology, biology and the marine environment. Graham and Trotman, London. 293 pp.

Hovland, M., Talbot, M., Olausen, S., Aasberg, L., 1985. Recently formed methane-derived carbonates from the North Sea floor. In: Thomas, B.M. (Ed.), Petroleum Geochemistry in Exploration of the Norwegian Shelf Norwegian Petrol. Soc. Graham & Trotman, London, pp. 236–266.

Hovland, M., Croker, P.F., Martin, M., 1994. Fault-associated seabed mounds (carbonate knolls?) off western Ireland and North-west Australia. Marine and Petroleum Geology 11 (2), 232–246.

Hovland, M., Gallagher, J.W., Clennell, M.B., Lekvam, K., 1997. Gas hydrate and free volumes in marine sediments: example from Niger delta front. Marine and Petroleum Geology 14 (3), 245–255.

Ingram, G.M., Eaton, S., Regtien, J.M.M., 2000. Cornea case study: lessons for the future. APPEA Journal 40 (1), 56–65.

James, N.P., Bone, Y., Kyser, T.K., Dix, G.R., Collins, L.B., 2004. The importance of changing oceanography in controlling Late Quaternary carbonate sedimentation on a high-energy, tropical oceanic ramp: north-western Australia. Sedimentology 51, 1179–1205.

Jeong, K.S., Cho, J.H., Kim, S.R., Hyun, S., Tsunogai, U., 2004. Geophysical and geochemical observations on actively seeping hydrocarbon gases on the south-eastern Yellow Sea continental shelf. Geo-Marine Letters 24, 53–62.

Jones, A.T., Logan, G.A., Kennard, J.M., Rollet, N., 2005a. Reassessing potential origins of synthetic aperture radar (SAR) slicks from the Timor Sea region of the Northern West Shelf on the basis of field and ancillary data. APPEA Journal 2005, 311–331.

Jones, A.T., Logan, G.A., Kennard, J.M., O'Brien, P.E., Rollet, N., Sexton, M., Glenn, K.C., 2005b. Testing natural hydrocarbon seepage detection tools on the Yampi Shelf, northwestern Australia, Geoscience Australia Survey S267. Post Survey Report: GA Record 2005/15, pp. 1–50.

Judd, A., 2001. Pockmarks in the UK sector of the North Sea. Technical report TR-002 produced for Strategic Environmental Assessment—SEA2 (dti), 70pp.

Judd, A.G., Hovland, M., Dimitrov, L.I., Garcia, G., Jukes, V., 2002. The geological methane budget at continental margins and its influence on climate change. Geofluids 2, 109–126.

Karisiddaiah, S.M., Veerayya, M., 2002. Occurrence of pockmarks and gas seepages along the central western continental margin of India. Current Science 82 (1), 52–57.

Keall, J.M., Smith, P.M., 2000. The impact of late tilting on hydrocarbon migration, eastern Browse Basin, Western Australia. AAPG Bulletin 84 (9), 1445–1446.

Keep, M., Moss, S., 2000. Basement reactivation and control of Neogene structures in the Outer Browse Basin, North West Shelf. Exploration Geophysics 31, 424–432.

Keep, M., Clough, M., Langhi, L., 2002. Neogene tectonic and structural evolution of the Timor Sea region, NW Australia. WABS 3, 342–353.

Kruglyakova, R.P., Byakov, Y.A., Kruglyakova, M.V., Chalenko, L.A., Shevtsova, N.T., 2004. Natural oil and gas seeps on the Black Sea floor. Geo-Marine Letters 24, 150–162.

Lavering, I., Jones, A., 2001. Carbonate Shoals and Hydrocarbons in the Western Timor Sea. PESA News 55, 40–42.

Leifer, I., 2003. Temporal and spatial variability in marine hydrocarbon seepage: implications for global estimates. AAPG Annual Meeting: Energy—Our Monumental Task Technical Program.

Leifer, Judd, 2002. Oceanic methane layers: The hydrocarbon seeps bubble deposition hypothesis. Terra Nova 16, 417–425.

Logan, G.A., 2004. Hope surfaces with gas bubbles in seep detection trial. AUSGEO News 75, 26–28.

Longley, I.M., Buessenschuett, C., Clydsdale, L., Cubitt, C.J., Davis, R.C., Johnson, M.K., Marshall, N.M., Murray, A.P., Somerville, R., Spry, T.B., Thompson, N.B., 2002. The North West Shelf of Australia—a Woodside perspective. In: Keep, M., Moss, S.J. (Eds.), The Sedimentary Basins of Western Australia 3: Proceedings of PESA Symposium, Perth pp. 27–88.

Loseth, H., Wensaas, L., Arntsen, B., Hovland, M., 2003. In: Van Rensbergen, P., Hillis, R.R., Maltan, A.J., Morley, C.K. (Eds.), Gas and fluid injection triggering shallow mud mobilization in the Hordaland Group, North Sea Geological Society, London, Special Publications, vol.216, pp. 139–157.

Marshall, J.F., Davies, P.J., Mihut, I., Troedson, A., Bergerson, D., Haddad, D., 1994. Sahul shoals processes: neotectonics and cainozoic environments—cruise 122. Post Cruise Report. Australian Geological Survey Organisation, Canberra.

Merewether, R., Olsson, M.S., Lonsdale, P., 1985. Acoustically detected hydrocarbon plumes rising from 2-km depths in Guaymas Basin, Gulf of California. Journal of Geophysical Research 90 (B4), 3075–3085.

Nakada, M., Lambeck, K., 1989. Late Pleistocene and Holocene sea-level change in the Australian region and mantle rheology. Geophysical Journal 96, 497–517.

Nash, C., Belford, S., 1996. Browse Basin Project 2042 interpretation report, World Geoscience Corporation Limited report undertaken for Australian Geological Survey Organisation, June 1996 1996.

O'Brien, G.W., Glenn, K.C., 2005. Natural hydrocarbon seepage, sub-seafloor geology and eustatic sea-level variations as key determiners on the nature and distribution of carbonate build-ups and other benthic habitats in the Timor Sea, Australia. In: Russel, B.C., Larson, H.K., Glasby, C.J., Willan, R.C., Martin, J. (Eds.), The Beagle, Records of the Museums and Art Galleries of the Northern Territory. Supplement 1. Understanding the Cultural and Natural Heritage Values and Management Challenges of the Ashmore Region, pp. 31–42.

O'Brien, G.W., Woods, E.P., 1995. Hydrocarbon-related diagenetic zones (HRDZs) in the Vulcan Sub-basin, Timor Sea: recognition and exploration implications. APPEA Journal 35 (1), 220–252.

O'Brien, G.W., Higgins, R., Symonds, P., Quaife, P., Colwell, J., Blevin, J., 1996. Basement control on the development of extensional systems in Australia's Timor Sea: an example of hybrid hard linked/soft linked faulting. APPEA Journal 36 (1), 161–201.

O'Brien, G.W., Morse, M., Wilson, D., Quaife, P., Colwell, J., Higgins, R., Foster, C.B., 1999a. Margin-scale, basement-involved compartmentalisation of Australia's North-West Shelf: a primary control on basin-scale rift, depositional and reactivation histories. APPEA Journal 39 (1), 40–63.

O'Brien, G.W., Lisk, M., Duddy, I.R., Hamilton, J., Woods, P., Cowley, R., 1999b. Plate convergence, foreland development and fault reactivation: primary controls on brine migration, thermal histories and trap breach in the Timor Sea, Australia. Marine and Petroleum Geology 16, 533–560.

O'Brien, G.W., Lawrence, G., Williams, A., Webster, M., Wilson, D., Burns, S., 2000. Using integrated remote sensing technologies to evaluate and characterise hydrocarbon migration and charge characteristics on the Yampi Shelf, north-western Australia: a methodological study. APPEA Journal 40 (1), 230–255.

O'Brien, G.W., Lawrence, G., Williams, A., Webster, M., Cowley, R., Wilson, D., Burns, S., 2001. Hydrocarbon migration and seepage in the Timor Sea and Northern Browse basin North-West Shelf, Australia: An Integrated SAR, Geological and Geochemical Study. Australian Geological Survey Organisation Report and GIS. Record 2001/11.

O'Brien, G.W., Cowley, R., Quaife, P., Morse, M., 2002a. Characterising hydrocarbon migration and fault-seal integrity in Australia's Timor Sea via multiple, integrated remote sensing technologies. In: Schumacher, D., LeSchack, L.A. (Eds.), Applications of Geochemistry, Magnetics, and Remote Sensing AAPG Studies in Geology, No. 48 and SEG Geophysical References Series No. 11, pp. 393–413.

O'Brien, G.W., Glenn, K., Lawrence, G., Williams, A., Webster, M., Burns, S., Cowley, R., 2002b. Influence of hydrocarbon migration and seepage on benthic communities in the Timor Sea, Australia. APPEA Journal 42 (1), 225–240.

O'Brien, G.W., Lawrence, G., Williams, A., 2003a. Assessing controls on hydrocarbon leakage and seepage. World Oil 2003, 49–56.

O'Brien, G.W., Cowley, R., Lawrence, G., Williams, A., Webster, M., Tingate, P., Burns, S., 2003b. Migration, leakage and seepage characteristics of the offshore Canning Basin and Northern Carnarvon Basin: implications for hydrocarbon prospectivity. APPEA Journal, 149–166.

Prior, D.B., Doyle, E.H., Kaluza, M.J., 1989. Evidence for sediment eruption on deep sea floor, Gulf of Mexico. Science 243, 517–519.

Roberts, H.H., 2001. Improved geohazards and benthic habitat evaluations: digital acoustic data with ground truth calibrations. OCS Study MMS 2001-050. US Department of the Interior, Minerals Management Service, Gulf of Mexico OCS Region, New Orleans, LA, 116 pp.

Sager, W.W., Lee, C.S., Macdonald, I.R., Schroeder, W.W., 1999. High-frequency near-bottom acoustic reflection signatures of hydrocarbon seeps on the Northern Gulf of Mexico continental slope. Geo-Marine Letters 18 (4), 267–276.

Sager, W.W., MacDonald, I.R., Hou, R., 2003. Geophysical signatures of mud mounds at hydrocarbon seeps on the Louisiana continental slope, northern Gulf of Mexico. Marine Geology 198, 97–132.

Sager, W.W., MacDonald, I.R., Hou, R., 2004. Side-scan sonar imaging of hydrocarbon seeps on the Louisiana continental slope. AAPG Bulletin 88 (6), 725–746.

Schumacher, D., 2000. Surface geochemical exploration for oil and gas: new life for an old technology. The Leading Edge, 258–261.

Shaw, J., Courtney, R.C., Currie, J.R., 1997. Marine geology of St George's Bay, Newfoundland, as interpreted from multibeam bathymetry and back-scatter data. Geo-Marine Letters 17, 188–194.

Shell Development (Australia) Pty. Ltd., 2000. Seismic interpretation report Cornea 3D Survey, Browse Basin, WA-241-P, WA-265-P & WA-266-P. Unpublished report.

Spry, T.B., Ward, I., 1997. The Gwydion discovery: a new play fairway in the Browse Basin. APPEA Journal 37 (1), 87–104.

Stakes, D.S., Orange, D., Paduan, J.B., Salamy, K.A., Maher, N., 1999. Cold-seeps and authigenic carbonate formation in Monterey Bay, California. Marine Geology 159, 93–109.

Struckmeyer, H.I.M., Blevin, J.E., Sayers, J., Totterdell, J.M., Baxter, K., Cathro, D.L., 1998. Structural evolution of the Browse basin, North West Shelf: new concepts from deep-seismic data. In: Purcell, P.G., Purcell, R.R. (Eds.), The Sedimentary Basins of Western Australia 2: Proceedings of Petroleum Exploration Society of Australia Symposium, Perth, WA pp. 345–367.

Taylor, M.H., Dillon, W.P., Pecher, I.A., 2000. Trapping and migration of methane associated with the gas hydrate stability zone at the Blake Ridge Diapir: new insights from seismic data. Marine Geology 164, 79–89.

Van Andel, T.H., Veevers, J.J., 1967. Morphology and sediments of the Timor Sea. Bureau of Mineral Resources. Geology and Geophysics Bulletin 83.

Van Rensbergen, P., Poort, J., Kipfer, R., De Batist, M., Vanneste, M., Klerkx, J., Granin, N., Khlystov, O., Krinitsky, P., 2003. Near-surface sediment mobilization and methane venting in relation to hydrate destabilization in Southern Lake Baikal, Siberia. In: Van Rensbergen, P., Hillis, R.R., Maltan, A.J., Morley, C.K. (Eds.), Subsurface Sediment Mobilization. Geological Society, London, Special Publications, pp. 207–221.

Willis, I., 1988. Results of exploration, Browse Basin, North West Shelf, Western Australia. In: Purcell, P.G., Purcell, R.R. (Eds.), The North West Shelf, Australia: Proceedings of the Petroleum Exploration. Society of Australia Symposium, Perth, pp. 259–272.

Yin, P., Berné, S., Vagner, P., Loubrieu, B., Liu, Z., 2003. Mud volcanoes at the shelf margin of the East China Sea. Marine Geology 194, 135–149.

Yokoyama, Y., Lambeck, K., De Deckker, P., Johnston, P., Fifield, L.K., 2000. Timing of the Last Glacial Maximum from observed sea-level minima. Nature 406, 713–716.

Yusifov, M., Rabinowitz, P.D., 2004. Classification of mud volcanoes in the South Caspian Basin, offshore Azerbaijan. Marine and Petroleum Geology 21, 965–975.